Linköping Studies in Science and Technology
Dissertations No. 2210

A Co-Simulation Tool Applied to Hydraulic Percussion Units

Håkan Andersson

LINKÖPING UNIVERSITY

LINKÖPING UNIVERSITY
LINKÖPING UNIVERSITY ELECTRONIC PRESS

Errata

A Co-Simulation Tool Applied to Hydraulic Percussion Units
Håkan Andersson
https://doi.org/10.3384/9789179292096

In the dissertation, Figure 6 on page 15 was found to be incorrect and is to be replaced by the figure below:

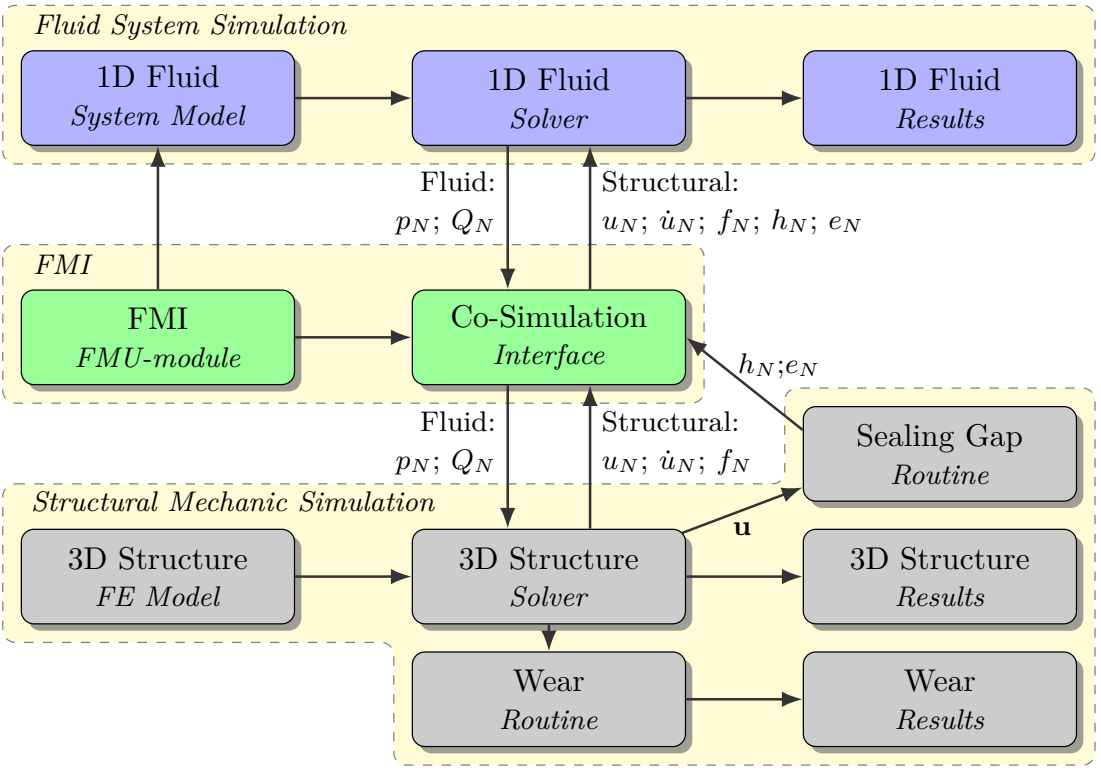

Linköping Studies in Science and Technology
Dissertations No. 2210

A Co-Simulation Tool Applied to Hydraulic Percussion Units

Håkan Andersson

Division of Solid Mechanics
Department of Management and Engineering
Linköping University
SE–581 83 Linköping, Sweden

Linköping, January 2022

Cover:
Front: The hydraulic hammer, the model and the results. Courtesy of Epiroc.
Background: The fluid system model in Hopsan.

Printed by:
LiU-Tryck, Linköping, Sweden, 2022
ISBN: 978-91-7929-250-8 (print)
ISBN: 978-91-7929-209-6 (PDF)
ISSN: 0345-7524
https://doi.org/10.3384/9789179292096

Distributed by:
Linköping University
Division of Solid Mechanics
Department of Management and Engineering
SE–581 83 Linköping, Sweden

This document was prepared with LaTeX, February 11, 2022

Preface

The work presented in this dissertation has been carried out at Epiroc, Kalmar, in collaboration with the Division of Solid Mechanics at Linköping Universtiy and Dynamore Nordic, Linköping. The financial support for this project has been completely provided by the Tools & Attachments division of Epiroc, which is gratefully acknowledged.

The work, which involved the areas of computer technology, fluid and solid mechanics and wear, has been of an interdisciplinary nature that challenged me to widen and deepen my knowledge within these areas, which has been most inspiring.

I would like to thank my supervisor Associate Prof. Daniel Leidermark for all his encouragement, patience and support throughout the project. I would also like to thank my other advisors at Linköping University; Prof. Kjell Simonsson and Assistant Prof. Joakim Holmberg for all their help during the project. Furthermore, I would like to thank my assistant advisors at Dynamore Nordic, Linköping; Dr. Daniel Hilding and Dr. Mikael Schill for their valuable knowledge they shared with me. A special thanks to Lic. Eng. Peter Nordin, co-author on my first paper, whos skills in technical programming and deep knowledge in the Hopsan simulation tool enabled the implementation of the co-simulation interface. I am also most grateful for the contribution of Dr. Thomas Borrvall who made the implementations of the co-simulation interface and the routines for the sealing gap in LS-DYNA. I would also like to thank my managers Erik Sigfridsson, Conny Sjöbäck and Olof Östensson who gave me the opportunity for Ph.D. studies and to carry out this research project. Finally, I would like to thank my family for their great support.

Håkan Andersson
Kalmar, January 2022

Abstract

In this dissertation, a co-simulation tool is presented that is meant to comprise a more comprehensive environment for modelling and simulation of hydraulic percussion units, which are used in hydraulic hammers and rock drills. These units generates the large impact forces, which are needed to demolish concrete structures in the construction industry or to fragment rock when drilling blast holes in mine drifting. This type of machinery is driven by fluid power and is by that dependent of coupled fluid-structure mechanisms for their operation. This tool consists of a 1D fluid system model, a 3D structural mechanic model and an interface to establish the fluid-structure couplings, which has in this work been applied to a hydraulic hammer. This approach will enable virtual prototyping during product development with an ambition to reduce the need for testing of physical prototypes, but also to facilitate more detailed studies of internal mechanisms.

The tool has been implemented for two well-known simulation tools, and a co-simulation interface to enable communication between them has been developed. The fluid system is simulated using the Hopsan simulation tool and the structural parts are simulated using the FE-simulation software LS-DYNA. The implementation of the co-simulation interface is based on the Functional Mock-up Interface standard in Hopsan and on the User Defined Feature module in LS-DYNA. The basic functions of the tool were first verified for a simple but relevant model comprising co-simulation of one component, and secondly co-simulation of two components were verified. These models were based on rigid body and linear elastic representation of the structural components. Further, it was experimentally validated using an existing hydraulic hammer product, where the responses from the experiments were compared to the corresponding simulated responses. To investigate the effects from a parameter change, the hammer was operated and simulated at four different running conditions.

Dynamic simulation of the sealing gap, which is a fundamental mechanism used for controlling the percussive motion, was implemented to further enhance the simulated responses of the percussion unit. This implementation is based on a parametrisation of the deformed FE-model, where the gap height and the eccentric position are estimated from the deformed geometry in the sealing gap region, and then the parameters are sent to the fluid simulation for a more accurate calculation of the leakage flow.

Wear in percussion units is an undesirable type of damage, which may cause

significant reduction in performance or complete break-down, and today there are no methodology available to evaluate such damages on virtual prototypes. A method to study wear was developed using the co-simulation tool to simulate the fundamental behaviour of the percussion unit, and the wear routines in LS-DYNA were utilised for the calculation of wear.

Populärvetenskaplig sammanfattning

I denna avhandling presenteras ett co-simuleringsverktyg som är tänkt att utgöra grunden för en simuleringsmiljö för att modellera och simulera hydrauliska slagverk som används i hydrauliska hammare och bergborrmaskiner. Sådana enheter används för att generera de stora krafterna som krävs för att krossa betongstrukturer vid rivningsarbete inom byggindustrin eller för att krossa berg vid borrning av spränghål vid gruvdrift. Dessa typer av maskiner drivs av hydraulik vilket innebär att kopplade fluid-strukturmekaniskmer ligger till grund för dess funktion, varför simuleringen av sådana mekanismer utgör kärnan i detta arbetet. Co-simuleringsverktyget består av en 1D fluidsystemmodell, en 3D strukturmekanikmodell och ett interface för att skapa fluid-strukturkopplingarna, och i detta arbete har en hydraulhammare använts för att demonstrera och validera dess funktionalitet. Detta verktyg kommer att möjligöra en simuleringsdriven produktutveckling med en ambition att reducera behovet av provning av fysiska prototyper, men det kommer också att ge förutsättningar för mer detaljerade studier av interna mekanismer.

Verktyget har implementerats för två välkända simuleringsprogram, och för att möjliggöra kommunikationen mellan dessa utvecklades ett co-simuleringsinterface. Simuleringen av enhetens hydrauliska funktion genomförs i systemsimuleringsverktyget Hopsan och strukturdelen simuleras i LS-DYNA, ett finita elementprogram. Co-simuleringsinterfacet är baserat på standarden Functional Mock-up Interface mot Hopsan, och på User Defined Feature modulen i LS-DYNA. Verktygets grundläggande funktionalitet verifierades med hjälp av enkla modeller som representerar slagverkets grundläggande mekanismer. Funktionaliteten verifierades först för co-simulering av en komponent och sedan för co-simulering av flera komponenter, vilket är ett krav då slagverket består av flera rörliga delar. De strukturella delarna i dessa modeller simulerades dels som helt stela och dels som helt elastiska för att successivt öka komplexiteten hos modellen. Vidare genomfördes en mer omfattande validering baserad på experimentella mätningar på en kommersiellt tillgänglig hydraulhammare. Dennna validering bestod av jämförelser mellan experimentella och simulerade resultat, och utifrån denna kunde man konstatera att simuleringsmetoden ger en god överensstämmelse inte bara för de grundläggande mekanismerna utan också för de mekanismer som är kopplade till vågutbredning i fluiden och strukturen. För att undersöka effekterna av en parameterförändring genomfördes experiment där hydralhammaren kördes vid fyra olika arbetsvillkor, och därefter jämfördes resultaten med simulerade resultat från motsvarande arbetsvillkor.

Tätningsspalten är en fundamental mekanism hos slagverket och den används för att styra den grundläggande rörelsen hos slagverket. Funktioner och rutiner utvecklades och implementerades i verktyget för att ge förutsättningar för en kopplad fluid-struktursimulering av dynamiska tätningsspalter, med en ambition att förbättra beräkningen av läckageflödet genom spalten. Implementationen är baserad på en rutin som parametriserar den deformerade FE-modellen vid tätningsspalten och beräknar spalthöjd och det excentriska läget, vilka sedan skickas till fluidsimuleringen för att användas vid beräkning av läckageflödet.

Slitage i slagverk är en oönskad skademekanism som kan resultera i försämrad prestanda eller orsaka allvarliga haveri, vilka kan ge upphov till produktionsbortfall. Då metodik för att studera sådana skador saknas för virtuella prototyper i dagsläget, presenteras i denna avhandling ett förslag på hur sådana mekanismer kan analyseras genom simulering. Metoden baseras på att simulera slagverkets fundamentala mekanismer med hjälp av co-simuleringsverktyget och i den efterföljande analysen används slitagerutinerna i LS-DYNA för att beräkna slitaget.

List of papers

In this thesis, the following papers have been included:

I. H. Andersson, P. Nordin, T. Borrvall, K. Simonsson, D. Hilding, M. Schill, P. Krus, D. Leidermark (2017). A co-simulation method for system-level simulation of fluid–structure couplings in hydraulic percussion units, *Engineering with Computers*, Volume 33, Issue 2, Pages 317-333

II. H. Andersson, K. Simonsson, D. Hilding, M. Schill, D. Leidermark (2017). System level co-simulation of a control valve and hydraulic cylinder circuit in a hydraulic percussion unit, *Proceedings of 15:th Scandinavian International Conference on Fluid Power, June 7-9, 2017, Linköping, Sweden*, Linköping University Electronic Press, Linköping University, Issue 144, Article Number 22

III. H. Andersson, K. Simonsson, D. Hilding, M. Schill, E. Sigfridsson, D. Leidermark (2019). Validation of a co-simulation approach for hydraulic percussion units applied to a hydraulic hammer, *Advances in Engineering Software*, Volume 131, Pages 102-115

IV. H. Andersson, L.J. Holmberg, K. Simonsson, D. Hilding, M. Schill, T. Borrvall, E. Sigfridsson, D. Leidermark (2021). Simulation of leakage flow through dynamic sealing gaps in hydraulic percussion units using a co-simulation approach, *Simulation Modelling Practice and Theory*, Volume 111, Article Number 102351

V. H. Andersson, L.J. Holmberg, K. Simonsson, D. Hilding, M. Schill, D. Leidermark (2021). Simulation of wear in hydraulic percussion units using a co-simulation approach, *Submitted*.

Note
The published appended papers have been reprinted with the permission of the respective copyright holders and all appended papers have been reformatted to the layout of the dissertation.

Own contribution
I have had the main responsibility regarding the analysis, the development work and the writing of the appended papers. **Paper I** is a collaboration with Lic. Eng. Peter Nordin, former Ph.D. student at the Division of Fluid and Mechatronic Systems, Linköping University, who was responsible for writing the section on the

Implementation. **Papers II – V** were entirely made by me with support from my co-authors. The development of the code for the co-simulation interface, the communication library and the FMU-generator, have been done by Peter Nordin. The LS-DYNA implementation of the co-simulation interface was done by Dr. Thomas Borrvall at Dynamore Nordic AB, Linköping. Dr. Borrvall also made the LS-DYNA implementation related to the dynamic sealing gap, which was presented in **Paper IV**. The experiments in **Paper III** was performed in collaboration with Kenneth Johansson Birath, Epiroc, Kalmar, while the data analysis was made by me. The experiment and the documentation of wear damages in **Paper V** was performed by Magnus Karlsson, Epiroc, Kalmar.

Contents

Part I

Application and method

1 Introduction

The trend of moving towards model based design has been strong within, e.g., the aerospace or automotive industry for many years, but has for the general machine building industry been hindered due to the lack of appropriate simulation tools. Other drivers such as new requirements from legislation on robustness, sustainability and environmental impact also requires that new products are evaluated at the product development phase using model based tools to a higher degree than today. Computer aided product development enables virtual prototyping which aims at reducing the need for physical testing of prototypes. Within the area of hydraulic percussion units that is intended for hydraulic hammers and rock drills, the strive for developing suitable simulation tools to be used for product development has been a continuous process over the last 30 years. These types of equipment are driven by fluid power and their function is completely dependent on coupled fluid-structure mechanisms. Hence, such machines requires a simulation tool where the coupled mechanisms can be represented well enough. This might be a demanding task because the characteristic of the mechanisms are of a short duration and high in magnitude, which will induce wave propagation throughout the model that needs to be resolved by such a tool. Another important mechanism is the interaction between the structural parts due to contact, which often is of a complex nature and needs to be handled correctly and efficiently. Furthermore, evaluation of stresses in the context of fatigue and durability, wear or predictions of radiated noise requires that structural responses are simulated for a 3D representation of the geometry.

Modelling of percussion units started in the 1990s, where the studies by Gorodilov [1–8] are among the first to study hydraulic impact machines by the use of mathematical models. Modelling of the percussive drilling process has a somewhat longer history than the hydraulic hammer application, where studies from the 1960s may be found. Studies of hydraulic percussion units by the use of the system simulation tool Amesim [9] are presented in the papers by Giuffrida and Laforgia [10], Ficarella et al. [11–13] and Oh et al. [14]. In those studies, the fluid system were represented by a network of 1D fluid components such as cavities, orifices and valves, and the structural parts were integrated in the same network by use of 1D mechanical components such as rigid body masses and springs. The fluid-structure couplings were modelled using a cylinder component, where the conversion of power between the fluid and structural domain happened. These types of models will represent the main function and the overall performance quite well because the main coupled fluid-structure mechanism is represented by the cylinder component. However, the wave propagation mechanism is only represented

on the system level and not at all on the component level, because internal wave propagation is not implemented for those components. To simulate responses that correspond to the real mechanisms to a higher degree the elastic behaviour of the structure and the fluid must be incorporated, which enables internal wave propagation on a component level.

The Fluid-Structure Interaction (FSI) method would meet a large part of the requirements for a simulation tool for hydraulic percussion units and this method is nowadays implemented in many software suits, such as ANSYS [15] and LS-DYNA [16]. This method is used for high fidelity co-simulation of 3D Finite Element (FE) models and 3D Computational Fluid Dynamics (CFD) models and is used to study coupled phenomena at a detailed level. However, one big disadvantage of this method is that it require large computational resources, hence it is not appropriate for transient simulation of models representing complete systems involving complex mechanisms. Large scale industrial use of FSI-simulations are presented in, e.g., [17, 18], but in general the applications can be found within the highly advanced industry of defence, aerospace and nuclear, which owns the computer resources needed to perform these simulations. This fact make it evident that other methods, which is less computational expensive, must be considered when modelling and simulating percussion units.

An alternative approach would be to model the fluid system using a simplified method, to incorporate the wave propagation. The demand of computationally inexpensive methods for co-simulation is evident when the response of the complete system are to be simulated within industries, with limited computer resources. But such methods can also be of interest for various parameter studies, such as sensitivity or optimisation studies, where a large number of simulations shall be performed the computer resources needed for each simulation will be of high interest. It has been shown that simplified methods based on 1D representations of fluid systems can be used to simulate the functional behaviour of complex systems, where the wave propagation in the sub-components are modelled by 1D partial differential equations [19].

The FE-method would be appropriate based on the above mentioned model requirements for the structural parts. This method is convenient when transient simulations of complex structural mechanisms, including contacts, shall be performed. The fluid-structure couplings could be established by co-simulation between a 1D fluid system model and a 3D structural FE-model. Co-simulation today must be regarded as a mature technique for simulation of coupled systems, where the couplings will affect the response in the systems significantly. Co-simulation can be set up for different type of models, e.g., 1D system models from different domains or for a 1D system simulation model and a 3D model, which represent a limited part of the system in more details, where the 1D-simulation provides the proper boundary conditions in the 3D-simulation at a low computational cost. A co-simulation between a 1D fluid system model and a 3D structural model will decrease the required computer resources, since a complete 3D CFD-model of the fluid system is far more computationally expensive than the 1D-model. Connecting 1D and 3D models have been done in several studies where models from different domains

and of different levels of complexity have been coupled [20–23]. Further, a full 3D structural response can also be utilised for stress analysis, assessment of fatigue, wear analysis, simulation of radiated noise etc. In the literature several studies are found using this approach, see, e.g., [24–26]. A co-simulation procedure for the general case is schematically shown in Fig.1.

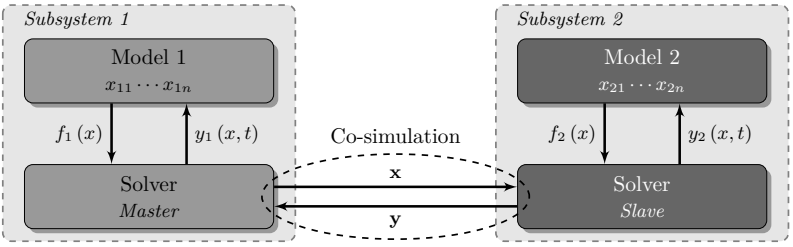

Figure 1: The co-simulation procedure of two subsystems. The parameters and functions $f_n(x)$ are sent to the simulator for each model. During the simulation the specified information, i.e. $\mathbf{x}$, $\mathbf{y}$, is exchanged between the simulators, thus affecting the response y_n in each model. Redrawn from Andersson [27].

Co-simulation of different types are today available through different software suits using there own technique, e.g., LS-DYNA [16] and ANSYS [15], but it has also been promoted by the Modelica Association and the Functional Mock-up Interface (FMI) standard [28], which many simulation software support. This is a free standard which defines an Functional Mock-up Unit (FMU) to exchange dynamic models or to set up co-simulation between modelling and simulation tools. Furthermore, a co-simulation approach will be flexible and versatile because it is possible to incorporate other simulation tools that may be needed to model other mechanisms.

When modelling fluid power machinery the fundamental mechanisms must be well represented, which could be done by using the co-simulation approach that has been described above. Additionally, there are also other important mechanisms in these machines that may be incorporated into the model to enhance the simulated responses and to enable detailed studies. The sealing gap is one such mechanism that is common within fluid power machinery and is also known in the literature as leakage gaps, clearance gaps or lubricating interfaces. There are a number of studies where radial piston machines have been analysed and where the sealing gaps have been modelled with the aim of predicting losses due to leakage [29–34]. Kamaraj et al. [35, 36] studied the leakage flow over the piston in a fuel injection pump, and Thiagarajan et al. [37] analysed the lateral leakage flow over a sealing gap in an external gear machine.

Another important mechanism in fluid power machinery is wear, which may cause damages that have a large influence on performance and life of the main internal components and it ranges from small scratches to severe adhesive wear that will cause a complete breakdown. Today, wear damages are evaluated on physical prototypes of the percussion unit because there is no established method to simulate

wear. The work of Ohmae and Tsukizoe [38] are among the first studies of wear using an FE-based method, which was published in the 1980s. They studied the sliding wear of an aluminium material by implementing an elasto-plastic material law in the FE-software which can be used to investigate the formation of sub-surface cracks that occur during adhesive wear. In the study by Põdra and Andersson [39] the wear was calculated using an Archard type [40] wear law where the contact pressure from the FE-simulation were used as input. The proposed method was validated against experimental results from a spherical pin-on-disc unlubricated tribology test and further applied to three different types of cone-on-cone spinning contact situations. A fairly large standard deviation was found for the absolute wear, but the method may rather be used for comparisons of different designs. In the paper by Borrvall et al. [41] functionalities for simulating wear for forming tools using LS-DYNA were presented. The default functions are based on an Archard type [40] wear law, but other wear laws may be implemented through the user defined wear interface. In the work by Puryear et al. [42] the wear routines, of the Archard type, in LS-DYNA were used to study wear of machinery components in buildings. In that study, the wear from three different material combinations were simulated to identify the most promising candidate. Methods for simulating wear for percussion units would facilitate assessments of wear on virtual prototypes, which in turn would save time and resources.

1.1 Aim of this work

The main objective of this work was to develop a co-simulation tool for hydraulic percussion units that incorporates the coupled fluid-structure mechanisms efficiently and that enable model-based design assessments at the product development phase. An additional objective was to allow for capabilities of model-based assessments of other mechanisms that can not be represented by the simulation tools that are used today, such as wear. The following research questions have been in focus throughout the work:

RQ1: Is it possible to establish a communication procedure for co-simulation of a 1D fluid system model and a 3D structural FE-model?

RQ2: Is it possible to co-simulate multiple components?

RQ3: Is it possible to replicate the real responses of a percussion unit using the co-simulation tool?

RQ4: Is it possible to utilise the elastic deformations of the FE-model to enhance the simulation of the sealing gap mechanism?

RQ5: Is it possible to simulate wear in percussion units using the co-simulation tool?

1.2 Outline

In Chapter 2, an introduction to hydraulic percussion units in the application of hydraulic hammers and rock drills is given. Furthermore, the percussion mechanism and the essential mechanisms are also presented. The co-simulation tool is presented in Chapter 3, together with the features developed and the underlying theory. Chapter 4 contains the validation of the co-simulation tool, where the experimental setups and the simulation models that were used to replicate the experimental results are presented. A simulation based verification of the method for simulating dynamic sealing gaps is also presented in this chapter. In Chapter 5 each of the appended paper is presented through short summaries. The main conclusions from the work and an outlook on future research subjects is presented in Chapter 6. Part II contains the five papers produced in this project.

2 The hydraulic percussion unit

Hydraulic percussion units may be found in equipment in the mining and construction industry, such as hydraulic hammers and hydraulic rock drills, where typical applications are to drill blast holes in rock material or to demolish concrete structures. These types of hard materials need high impact forces to be crushed or fragmented, and further the number of impacts per time unit is essential for productivity reasons. The two properties, i.e. the impact force magnitude and the impact frequency, are the main advantages of the hydraulic percussion unit, and are conveniently generated by the percussive mechanism.

The hydraulic hammer, see Fig. 2, was developed and launched for serial production in the 1960s, and today it is used in many different applications such

(a) **(b)**

Figure 2: (a) An excavator with a hydraulic hammer at a typical work site demolishing concrete structures, and (b) the Epiroc SB202 hydraulic hammer. Courtesy of Epiroc.

as demolition, deconstruction, primary rock excavation, secondary rock breaking, foundation work, asphalt cutting and trenching. The hammers are produced in a wide range of different sizes, from 50 to 10000 kg may be found on the market today, where the smaller are used for light renovation work and the larger models are used in quarries for secondary breaking of boulders, primary excavation of softer rock can also be found. The most common situation is to assemble the hammer on an ordinary excavator and connect it to the hydraulic system of the excavator, which then supply the percussion unit with hydraulic power. Typical properties of hydraulic hammers are listed in Table 1.

The first rock drills invented in the 1850s were powered by steam, and later in the 19th century also by compressed air. The hydraulic rock drill was invented in the 1920s and was driven by water, and the main application was oil and water well drilling. In the early 1970s rock drills powered by oil hydraulics were launched on the market. Common applications today for rock drills are blast hole drilling when driving tunnels or in mine drifting. Special drill rigs are needed to maximise the performance of the rock drill, and these must be able to generate the feeding force needed and to supply the demanded hydraulic power. An example of a drill rig for mine drifting is shown in Fig. 3a, and a rock drill are shown in Fig. 3b. Typical properties of rock drills are listed in Table 1.

(a)

(b)

Figure 3: (a) A drill rig at the face, drilling blast holes in a mine and (b) the Epiroc COP MD20 hydraulic rock drill. Courtesy of Epiroc.

Table 1: Characteristic properties of the Rock drill and the Hydraulic hammer.

	Operating pressure	Oil flow	Impact Energy	Impact Frequency
Rock Drill	High	High	Medium	High
Hydraulic Hammer	Medium	Medium	High	Low

2.1 Percussion mechanism

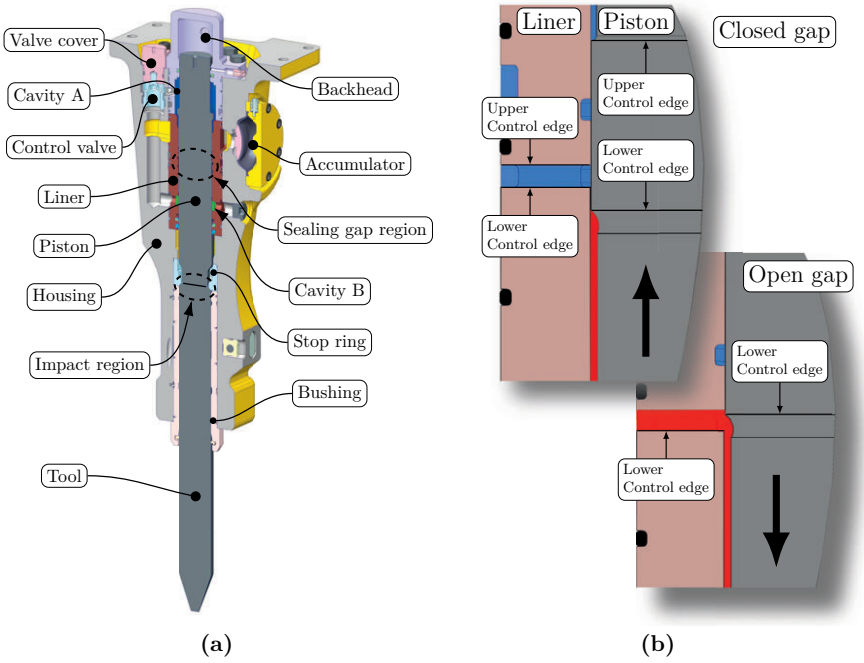

Figure 4: Components and features in the percussion unit (a) of a hydraulic hammer and (b) the sealing gap mechanism; the upper illustration shows a closed state and the lower shows an open state.

The two most important properties of the percussion unit are to generate high impact forces and high impact frequency, which are produced by the percussive motion of the piston. Depending a little bit on the working principle of the hydraulic hammer, but it typically consists of a number of components and features that defines the operation of the machine, and these are shown in Fig. 4a. The part where the hydraulic energy is converted to mechanical energy is the piston, which will be put into motion by the hydraulic pressure in the cavities A and B. The oil flow, and thereby the pressure level, in these cavities is controlled by the control valve, which in turn is controlled by a valve mechanism that is formed between the piston and the liner, i.e. the sealing gap region in Fig. 4a. This valve mechanism is known as the sealing gap mechanism and is a fundamental element for the operation of the percussion unit, see Fig. 4b. Furthermore, the piston is guided by the liner that also contain sealings to prevent oil leakage from the hydraulic part of the hammer. On the upper side, the hammer is sealed off by the backhead and the

valve cover. The outer casing of the hammer is labelled Housing, in which all internal parts are assembled, further a number of channels for distribution of oil to the different cavities of the percussion unit exist.

The sealing gap acts as a valve mechanism and it can either be closed or opened for flow of oil in the percussion unit. In the upper illustration of Fig. 4b, the sealing gap is displayed at a closed position, but as the piston move upwards the lower gap will open, see the lower illustration of Fig. 4b, and oil will be permitted to flow from the high pressure region, red area, to the low pressure region, blue area. At this phase, the lower control edge on the piston is positioned above the lower control edge on the liner, hence the lower sealing gap is open. The same sequence occurs for the upper control edges when the piston is moving downwards. Even if the sealing gap is closed a small leakage flow will occur, which by part is due to the clearance between the piston and the liner. This is the main mechanism for the sealing gap, but it has a few other important functions as well, which is presented in Section 3.3.

A typical percussive motion for the piston is presented in Fig. 5, showing three complete working cycles and the different phases, i.e. the return and the working stroke. The time scale is normalised to the impact frequency, which is calculated as

$$f = \frac{1}{\overline{\Delta t_i}} \tag{1}$$

where $\overline{\Delta t_i}$ is the average time interval between each impact, resulting in an interval of unity, further the position is normalised against the stroke length Δu_p and the position of impact is set to zero.

The working cycle starts at $t = 0$ in Fig. 5 and at this point the piston is resting on the top of the tool, further the control valve is closed, which results in a low pressure level in cavity A. The pressure level in cavity B is held at a high level throughout the complete operation of the unit, except for some dynamic fluctuations. The pressure difference in the cavities together with different sizes of the piston control areas creates an upward resultant force, which will put the piston into motion and carry out the return stroke. A short while before the piston reaches the upper turning point, the control valve will open and thereby pressurise cavity A at a high level, which first will stop the upward motion of the piston, and secondly will accelerate it towards the tool, and this is the starting point of the working stroke. At this point the lower sealing gap on the piston will open to enable high pressurised oil to flow to the control valve, which by that is forced to the opened position. At this phase the pressure is on the same level for both cavities, but due to the larger pressurised area on the piston in cavity A, a downward resultant force is generated. Furthermore, during the working stroke the required oil flow into cavity A is higher than what can be delivered from the hydraulic system of the carrier, and to prevent an unwanted pressure drop oil is temporarily delivered from the accumulator. Eventually the piston will impact the tool, and the kinetic energy of the piston is transferred to the tool by generating a stress wave, which is transmitted through it and will break the material at the tip of the tool. During

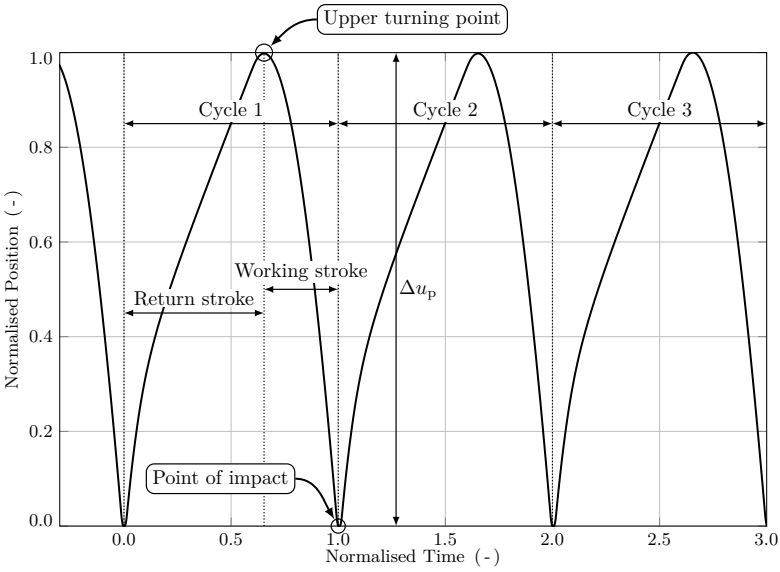

Figure 5: A normalised piston motion of a hydraulic hammer. The working cycle consists of the return stroke, where the piston is lifted to the upper turning point, and the working stroke, where the piston is accelerated towards the tool and the point of impact. The stroke length Δu_p represents the difference in length between the impact position and the upper turning point.

the working stroke, a short distance before the impact occur the upper sealing gap on the piston will open to release the pressure on the control valve, which then closes and drain the pressure in cavity A, and the piston again is subjected to an upward resultant force ready for the next working cycle. The time of impact finish the working stroke and the working cycle, and the next cycle will start when the piston once again is moving upwards. Above, the working principle for the percussion unit used in this research project is described, but there are several other principles for such units, see for instance the study by Gorodilov [5] or by Giuffrida and Laforgia [10].

2.2 Essential mechanisms

As described in the previous section, the hydraulic percussion unit working process is of a reciprocating nature, which is controlled by alternating the pressure levels in the cavities surrounding the moving components. During the working stroke the piston is accelerated downwards by the fluid pressure and when it suddenly stops at impact, pressure waves will be generated in the fluid since the fluid still is in motion and will initiate a transient increase of pressure against the stationary wall of the piston, which also is known as the water hammer effect [43]. Abrupt changes

in oil flow also occurs when the different valve mechanisms in the percussion units opens and closes, which also will generate pressure waves in the fluid system. These waves affects the components on a local level and may cause damages from erosion and cavitation, but they may also influence the overall performance.

Similar mechanisms occur in the structural parts, i.e. when the piston is impacting the tool stress waves are generated. The primary wave in the tool is carrying the main energy to the tip, where it partly are dissipated to break the material, the non-used energy is reflected at the tip and will be transmitted to the top of the tool. At the top of the tool the stress wave partly is transferred to the piston and the residual energy is transferred to the housing via the stop ring. In general, the stress wave contains a lot of energy and high contact forces are generated, these may cause damages such as wear and fatigue and will also generate vibration and noise. Since these short duration mechanisms are natural features of the percussion unit, and the main work of the machine are carried out by these, it is of most importance to consider the effects from these during design.

As mentioned above, the piston is guided by the liner if observed on a greater scale, but on a micro scale a thin oil film is formed between the piston and the liner. The oil film has several positive effects, it will force the piston to a concentric position due to the strive for equilibrium in the fluid, it prevents contact between the components, and by that friction and wear is reduced. It also introduce viscous dampening in the percussion unit, which is beneficial to reduce vibrations. As long as the main percussion mechanism in the axial direction is analysed, the properties of the oil film will be not that important, but when the lateral behaviour of the piston shall be analysed the oil film properties are crucial. Contact occur between the components if the lateral forces are larger than those generated by the oil film pressure. In this project two mechanisms, where the oil film properties come into play have been studied, the sealing gap mechanism and the sliding wear between the piston and the liner. For the leakage flow over the closed sealing gap, the concentric position of the piston is critical because the flow can be 2.5 times higher for a fully eccentric annulus gap. Hence, the lateral position of the piston, which is controlled by the oil film, is critical for the leakage flows in the percussion unit. For the second mechanism of sliding wear it is obvious that in principal no wear occur as long as an oil film is separating the components. Thus, it is important to study at which lateral force magnitude contact occurs, and also at which position, which to a large extent are determined by the oil film. In general, occurrence of wear in percussion units is highly damaging and it often cause critical failure or complete breakdown.

3 The co-simulation tool

The main outcome from this research project has been a co-simulation tool that primarily is intended for virtual prototyping and advanced analyses of hydraulic percussion units for design and evaluation. The tool contain three different main parts, the 1D fluid system simulation, the FMI, which include the co-simulation interface, and the 3D structural mechanic simulation, which also holds the features for simulating sealing gaps and wear. The utilised co-simulation approach is presented in **Paper I**, where the implementation of the tool is described. A schematic flow chart where the simulation features and the flow of information in the simulation tool is displayed in Fig. 6.

In the fluid system simulation, the pressure p is calculated and communicated through the co-simulation interface to the structural mechanic simulation, which in turn computes displacements u, velocities $\dot{u}$, forces f, gap heights h and eccentricities e. The structural variables are sent back to the fluid simulation for calculation of pressures and flows Q for the next time step, and then the procedure is repeated

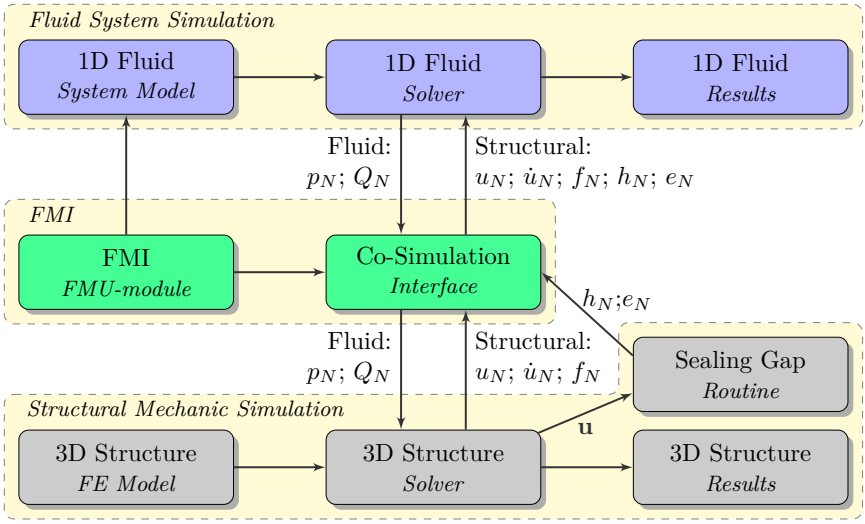

Figure 6: The overall simulation sequence. The index N refers to the identity of the co-simulation component. Figure from **Paper V**.

throughout the simulation. The results from the fluid system simulation facilitates not only analyses of system performance and efficiency on an overall level, but the fluid responses on the component level can also be analysed to some extent. The FE-results facilitate analyses of motions, stresses, fatigue, radiated noise, etc.

The simulation tool is implemented using the Hopsan simulation tool for the 1D fluid system simulation and the FE-software LS-DYNA for the 3D structural simulation. The interface is developed based on the Functional Mock-up Interface standard and the Functional Mock-up Unit is included in the fluid system model to incorporate the structural model. The FMI and FMU are further explained in Section 3.1. The fluid system is incorporated in the structural model by using the User Defined Feature (UDF) module in LS-DYNA.

In **Paper I** the tool was verified for simple but relevant models that involved co-simulation of one sub-component, and in **Paper II** it was further developed to facilitate co-simulation of N sub-components. The models that were used for verification in **Paper I** and **II** contained typical mechanisms of a percussion unit, while a complete model of a typical hydraulic hammer was used for validation against experimental responses in **Paper III**.

As described in Section 2.1, the sealing gap is a fundamental mechanism for the operation of the percussion unit, which operation depends on the fluid behaviour, the motion and the deformation of the structure. This by definition is a fluid and structure coupled mechanism and it was found appropriate to include this feature as the next step in developing the co-simulation tool. In **Paper IV** routines for simulating dynamic sealing gaps are presented, which aims to further enhance the simulated response of the percussion unit, see the Sealing Gap feature in Fig. 6. Furthermore, a method for evaluating wear in percussion units is presented in **Paper V**, which is related to the wear features in Fig. 6. The mechanisms that are studied in **Paper IV** and **V** are depending on the lateral behaviour of the piston, which to a large extent is controlled by the oil film that is formed between the components, see Section 2.2. In these studies the oil film was modelled using a strategy that is based on the Mortar contact routine in LS-DYNA, which is described in Section 3.4.

3.1 The Hopsan simulation tool

The Hopsan simulation tool is a 1D multi-domain simulation software primarily for simulation of fluid power and mechatronic systems, and is based on the Transmission Line Modelling (TLM) technique. It has been developed since the late 1970s by the Division of Fluid and Mechatronic Systems at Linköping University, and in the beginning of 2000 it was subjected to a complete re-programming using the object oriented language C++, which was launched 2010 as the Hopsan Next Generation [44]. Historically, Hopsan has been one of the most important tool for developing hydraulic percussion units within Epiroc, mainly because of the short time for simulation and the proper handling of the pressure waves in the fluid system. These features are facilitated by the use of the TLM-technique. The

Hopsan simulation tool is described in more detail by for instance Braun [45].

Hopsan utilise the concept of power ports at the connection points for the sub-components. This concept facilitate an intuitive approach to define physically related connection points for the transfer of power between sub-components, which in the real world can be represented by a hydraulic hose or an electric cable. For instance, in the fluid domain, the power is calculated by the pressure and the flow, while the velocity and the force are used for the mechanical domain.

Furthermore, Hopsan supports the FMI standard [28] for model exchange and co-simulation, which means that a complete Hopsan model can be exported as a sub-component to be integrated in a model built in another simulation system that supports the FMI standard for co-simulation and vice-versa. A sub-component that is exported from a modelling or simulation tool following the FMI standard is called a Functional Mock-up Unit and facilitates a standardised interface to be used for exchanging dynamic models.

3.1.1 Transmission line modelling method

An efficient method that can be used for the study of distributed physical systems, e.g., hydraulic, pneumatic or electric, and which is known as the TLM method was proposed by Auslander [46], who referred to this method as bilateral delay-line modelling. In this method, a time delay T is introduced that is physically motivated, which will decouple each sub-component in the system to facilitate individual simulation of each sub-component, which is essential when introducing parallel simulations. The time delay is determined from the wave propagation speed in each sub-component. The principal of time delay facilitates the use of weak couplings at the connection points and this approach makes it possible to solve the system using an explicit time integration method, in comparison to the implicit method that is more time consuming.

For the TLM component with the boundary conditions shown in Fig. 7 the governing equations can be written as

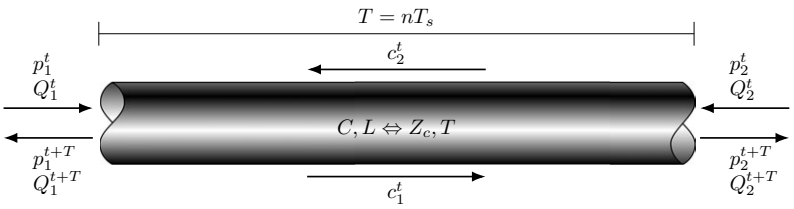

Figure 7: A pipe element containing a fluid with the pressure p and the flow Q as the boundary values on each side, which schematically represents a TLM component. Redrawn from **Paper I**.

$$p_2^{t+T} = c_1^t + Z_c Q_2^{t+T} \tag{2}$$
$$p_1^{t+T} = c_2^t + Z_c Q_1^{t+T}, \tag{3}$$

where the impedance Z_c and time delay T are given by the capacitance C and inductance L of the component according to

$$Z_c = \sqrt{\frac{L}{C}} \tag{4}$$
$$T = \sqrt{LC}, \tag{5}$$

and where the wave variables c are calculated as follows

$$c_1^t = p_1^t + Z_c Q_1^t \tag{6}$$
$$c_2^t = p_2^t + Z_c Q_2^t \tag{7}$$

The relation between the pressure and flow on each side of the TLM element are presented in the Eqs. 2 and 3. From these equations it is also evident that the pressure on one side depends on the pressure from the other side from the previous time step, and this behaviour produces the propagation of pressure waves through the component

Regarding applications of the TLM-method, the paper by Krus et al. [19], where the responses of a hydromechanical system was simulated, is worth mentioning, and further an in-depth presentation of the TLM-method is given by Braun [45]. The above mentioned studies are using the simulation tool Hopsan, which is a TLM-based simulation tool, which historically has been found to be an efficient tool for predicting the responses of hydraulic percussion units.

3.2 The LS-DYNA FE-software

The general-purpose finite element software LS-DYNA [16] is capable of simulating highly non-linear and short duration mechanisms, which are essential when simulating hydraulic percussion units. LS-DYNA originates from the DYNA3D FE-code that was developed by J.O. Hallquist at the Lawrence Livermore National Laboratory in the United States of America in 1976. The software was developed to facilitate stress analysis of structures subjected to short duration impact loading by an efficient element implementation and an efficient handling of contacts. In 1988 the Livermore Software Technology Corporation was founded to continue the development of DYNA3D, which was commercially launched as the LS-DYNA software in 1989. The explicit solver in LS-DYNA has been found to work very well when simulating hydraulic percussion units, which mainly are due to the handling of stress waves and part interactions by contact. In the percussion unit many different

types of contact occur, e.g., short duration contact, impact and sliding that needs to be handled efficiently.

In LS-DYNA, the general equation of motion is stated as

$$\mathbf{M}\ddot{\mathbf{u}} + \mathbf{C}\dot{\mathbf{u}} + \mathbf{f}_{\text{Int}} = \mathbf{f}_{\text{Ext}} \tag{8}$$

where $\mathbf{M}$ is the mass matrix, $\mathbf{C}$ is the damping matrix and $\mathbf{f}_{\text{Int}}$ is the internal force vector. The external force vector, $\mathbf{f}_{\text{Ext}}$, represents all external loads acting on the FE-model. The displacement $\mathbf{u}$ is solved explicitly by the central difference time integration scheme described by

$$\dot{\mathbf{u}}^{n+\frac{1}{2}} = \dot{\mathbf{u}}^{n-\frac{1}{2}} + \ddot{\mathbf{u}}^{n}\Delta t^{n} \tag{9}$$

$$\mathbf{u}^{n+1} = \mathbf{u}^{n} + \dot{\mathbf{u}}^{n+\frac{1}{2}}\Delta t^{n+\frac{1}{2}} \tag{10}$$

where Δt^n is the time step and based on this, it couples well with the TLM method. The explicit time integration scheme is described in more detail in the literature, see for instance the book by Belytschko et al. [47].

As already mentioned, Hopsan is supporting the FMI standard for co-simulation, while LS-DYNA do not, at least not until version R12. Hence, functionalities for a co-simulation interface for LS-DYNA needed to be developed. In LS-DYNA there is functionalities for customised external loads, i.e. User Defined Feature (UDF), which was decided to be used for accessing the FE-simulation. Furthermore, a library of functions for communication using the TCP/IP network protocol was developed to transmit the system simulation signals to the UDF. The utilisation of the TCP/IP communication facilitates a flexible setup of the computers for simulations, i.e. the co-simulation can be executed as long as each computer used for simulation belongs to the same network. The interface points for co-simulation in each model are defined in a common configuration file which is used both by the FMU-generator to build the FMU for Hopsan and by the UDF module in LS-DYNA. Further details on the co-simulation interface can be found in **Paper I**.

3.3 Sealing gap

The sealing gap is a vital element in the percussion unit because it controls the fundamental reciprocating mechanism of the piston. The main mechanism for the sealing gap is described in Chapter 2, while the implementation of the sealing gap is given in this section. Figure 8 presents a more detailed illustration of the sealing gap mechanism than Fig.4, and here is also an intermediate stage given in Fig. 8b. In Fig. 8a, the sealing gap is at the closed position and the piston is moving upwards. When the intermediate stage is reached, see Fig. 8b, the gap length l_{gap} has been reduced significantly, which will make the leakage flow increase. Eventually, the gap will open, see Fig. 8c, which happens when the control edge on the piston has moved above the control edge on the liner, to allow for, in principal, unrestricted

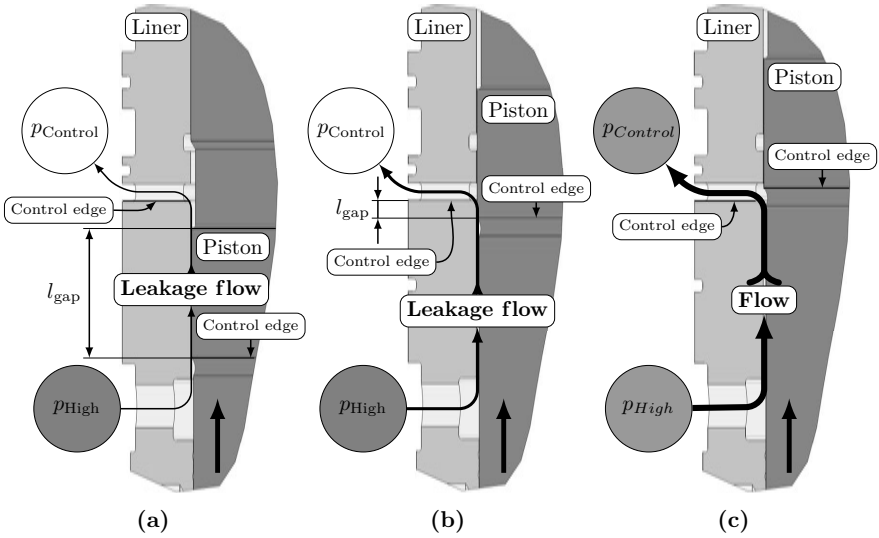

Figure 8: The sealing gap mechanism, showing the opening phase when the piston is moving upwards. At the closed stage (a) a small leakage flow is passing through the gap, at the intermediate stage (b) the leakage flow is somewhat larger due to the shorter gap length l_{gap} and the opened stage (c) where the fluid may flow freely between the pressure regions p_{High} and p_{Control}. The relative position of the control edges on the piston and on the liner determines the status of the sealing gap. Redrawn from **Paper IV**.

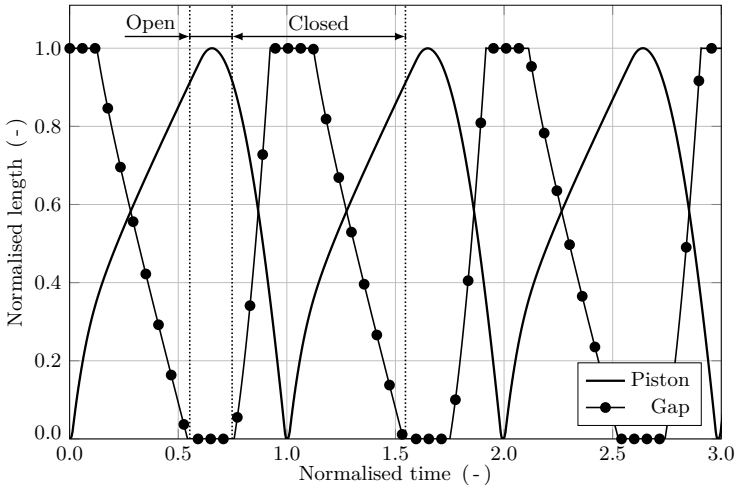

Figure 9: A typical normalised length of a sealing gap in relation to the piston motion.

flow and the pressure region p_{Control} will be pressurised. The sealing gap length l_{gap} is determined by the piston motion and a typical normalised length for a gap is shown in Fig. 9, where the gap is closed when Norm $l_{\text{gap}} > 0$ and opened at Norm $l_{\text{gap}} = 0$.

The cross section of the closed sealing gap at an eccentric position and the measures required to calculate the leakage flow is shown in Fig. 10. The gap height h for an annulus is defined as

$$h = r_{\text{c}} - r_{\text{p}}, \tag{11}$$

where r_{c} and r_{p} is the radius of the liner and the piston respectively. The index c refers to the Cylinder part of the annulus that for this case is designated as the Liner.

The leakage flow $Q_{\text{Leak Ecc}}$ for the eccentric annulus shown in Fig. 10, has among others been derived by White [48], and can be calculated according to

$$Q_{\text{Leak Ecc}} = \frac{\pi \Delta p}{8 \mu \, l_{\text{gap}}} \left[r_{\text{c}}^4 - r_{\text{p}}^4 - \frac{4e^2 A^2}{\beta - \alpha} - 8e^2 A^2 \sum_{n=1}^{\infty} \frac{n \, \text{e}^{-n(\beta+\alpha)}}{\sinh\left(n\beta - n\alpha\right)} \right], \tag{12}$$

where

$$A = \sqrt{B^2 - r_{\text{c}}^2} \ , \ B = \frac{r_{\text{c}}^2 - r_{\text{p}}^2 + e^2}{2e}, \tag{13a,b}$$

$$\alpha = \frac{1}{2} \ln \frac{B + A}{B - A} \ , \ \beta = \frac{1}{2} \ln \frac{B - e + A}{B - e - A}, \tag{13c,d}$$

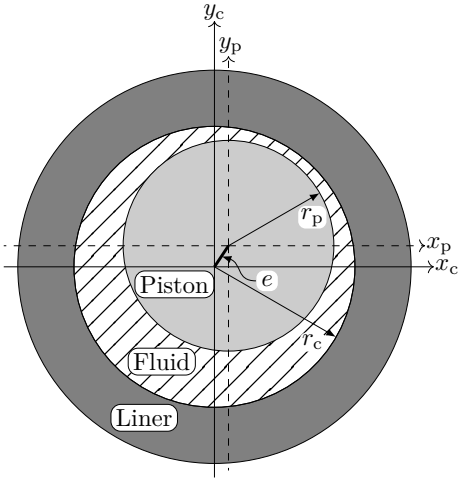

Figure 10: The cross section of a closed sealing gap where the piston is at an eccentric position. Figure from **Paper IV**.

and Δp is the pressure difference, e is the eccentric position and μ is the dynamic viscosity of the fluid.

For oil hydraulic applications the gap height commonly is much smaller than the piston diameter, and by using this assumption the ratio between the flow through an eccentric and a concentric annulus was derived by White [48] and is calculated according to

$$\frac{Q_{Leak\ Ecc}}{Q_{Leak}} = 1 + \frac{3}{2}\left(\frac{e}{h}\right)^2. \tag{14}$$

Furthermore, a simplified equation for the flow through a concentric annulus was derived by Massey [43] using the assumption above and can be calculated as

$$Q_{Leak\ simple} = \frac{\pi D_p h^3 \Delta p}{12 \mu l_{\text{gap}}}, \tag{15}$$

where D_{p} is the diameter of the piston. The geometrical dependencies for the leakage flow can be identified from Eq. 15 as being the gap height h and the gap length l_{gap}, where the gap height is the most critical because the flow is proportional to h^3. From Eq. 14 it may also be noticed that the flow for a maximum eccentric annulus, i.e. $e = h$, is 2.5 times higher than for the concentric position. In Hopsan the leakage flow through a closed sealing gap is calculated in two steps, first for the concentric position using Eq. 15 and secondly the flow is adjusted for the eccentric position using Eq. 14.

3.3.1 Implementation

The implementation of sealing gaps in this project is concentrated on extracting geometrical parameters for the gap by use of the FE-model, where a complete representation of the deformed geometry is available. Functions for the fluid simulation of the sealing gap are already implemented in Hopsan, and can be feed with dynamic values of the gap height and the eccentric position. The gap length is already implemented and simulated in Hopsan using the relative motion of the components in the fluid system model.

A routine to extract the geometrical variables from the deformed FE-model was developed and the details are presented in **Paper IV**. In short, the routine is based on fitting, in a least square sense, two cylindrical surfaces of the sealing gap region, one for the liner and one for the piston, and the gap height is calculated as the difference between the radius for each cylinder. Further, the axis for each cylinder is also calculated and the eccentric position is calculated as the difference in position between the axes. As an option, the gap length is determined from the end positions of the fitted cylinders, but this signal is not used here.

The co-simulation interface was extended to transmit the geometrical variables as signals from LS-DYNA to Hopsan during the simulation, see h_N and e_N in Fig. 6, by implementing a new type of signal. This signal is defined in the configuration file and is then recognised by the FMU-generator to add output signal ports to

the FMU, which can be connected to the corresponding gap in the fluid system model to simulate the dynamic sealing gap. On the LS-DYNA side, the UDF keywords are utilised to couple each sealing gap to the three segment sets that defines its geometrical region. The setup of the UDF invokes the parametrisation of the FE-result to extract the gap height and the eccentric position. Results from a simulation using dynamic sealing gaps are presented in Section 4.

3.4 Oil film modelling

In Chapter 2, the oil film that is formed between the piston and the liner is identified as an essential mechanism in the percussion unit, especially when lateral motions are to be studied. In the co-simulation tool, the oil film is modelled in the FE-model by using the Mortar type of contact in LS-DYNA, where functionalities for using prescribed contact pressures have been implemented in version R12. The contact routine keep track of the relative distance and speed between the contact surfaces and by a table look-up function the corresponding contact pressure value is interpolated from the specified curves and is applied to the segments in contact. The curves of prescribed contact pressure depend on the relative distance and the speed.

The oil film mechanism referred to in this application can in the literature be recognised as a Squeeze Film Damper (SFD), which have been the subject for

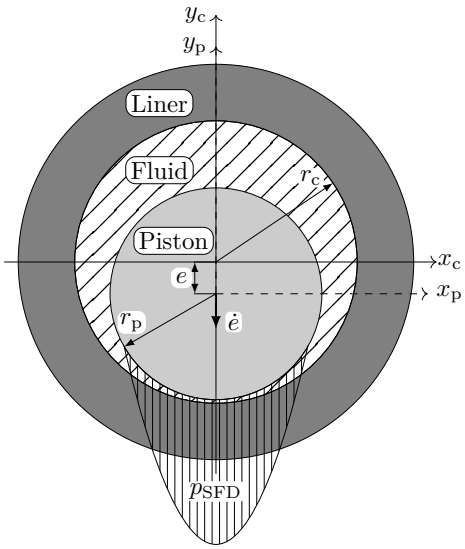

Figure 11: The oil film that is formed between the piston and the liner. The piston moves in the negative direction of y_p at the eccentric position e at the speed $\dot{e}$, which generates a total pressure in the oil film of p_{SFD}.

extensive research within the area of gas turbines, see for instance the study by Barrett and Gunter [49], where the oil film pressure was derived from the Reynolds equation and is calculated as

$$p_{\mathrm{SFD}} = \frac{\mu l^2 \left(2\varepsilon^2 + 1\right)}{4h^3 \left(1 - \varepsilon^2\right)^{5/2}} \dot{e}, \tag{16}$$

where l is the length of the fluid film, ε is the eccentricity ratio

$$\varepsilon = \frac{e}{h}, \tag{17}$$

and $\dot{e}$ the time derivative of the eccentric position that is the relative speed between the contact surfaces of the piston and the liner, for more details see Barrett and Gunter [49]. Eq. 16 has the characteristic to approach infinity as the eccentricity ratio advance toward unity, which may cause numerical issues within the FE-simulation. Such issues can be handled by introducing a maximum allowed contact pressure for large eccentricity ratios.

3.5 Wear

Wear damages are unfavorable for performance and lifetime in percussion units, and can ultimately cause complete breakdown. Today, wear is evaluated on physical prototypes which is a time consuming and resource demanding task. Wear can be initiated from sharp edges and corners that are insufficiently deburred in the manufacturing process, and such wear damages can often be eliminated by improving the deburring process, without any major design changes. However, the wear test must be repeated to verify the updated manufacturing process. Simulation of wear that is related to burrs or sharp edges is probably a delicate task because in general these are small and will require a much finer mesh in the FE-model than normally is used for models of percussion units. Apart from burrs, wear may also be initiated by fundamental elements in the design, such as the diameter to length ratio, or the distance between the guiding diameters. If wear is encountered during testing and is judged to originate from a poor fundamental design ratio a redesign of the involved components must be initiated. Such task is often hard to solve and is to a large extent dependent on the staff experience from similar designs. When the redesigned prototypes have been manufactured the wear test must be repeated to verify that no wear occur for the redesigned components. For such situations a method to simulate wear would be of great help.

A method to study wear on virtual prototypes is presented in **Paper V**, where the co-simulation tool is used to simulate the operation of the percussion unit and the wear is simulated utilising the wear routines in LS-DYNA. The information flow for simulating wear is displayed in Fig. 6 and is related to the wear features in the structural mechanic simulation. These routines are based on a post-processing of FE-results, where the sliding distance and the contact pressure of the surfaces in

contact are registered, thus no material is removed from the model during simulation. In this implementation, the wear rate $\dot{w}$ is calculated from the sliding speed $\dot{d}$ and the contact pressure p using a wear law of an Archard type [40] according to

$$\dot{w} = k\frac{p\dot{d}}{H} \tag{18}$$

where k is the wear constant and H is the hardness. The wear constant is determined for each contact situation and can for simple cases be found in the literature, but for high accuracy it shall be determined from tribology tests. The wear simulation is invoked by specifying the keyword CONTACT_ADD_WEAR in LS-DYNA, where the wear constant are specified for the specific contact situation and the hardness are specified for each material in the contact.

Furthermore, wear is closely related to the oil film between the piston and the liner that is presented in Section 3.4 and as long as the oil film is separating the components the wear will be negligible. Hence, the behaviour of the oil film must be properly represented to obtain realistic results when simulating wear.

4 Validation

In this research project, a co-simulation tool for detailed analyses of hydraulic percussion units has been developed. In **Paper I** and **II**, the functionality of the tool was verified for simple virtual models showing that the method is capable of representing the responses for such models. However, the results from a new simulation tool must be validated by more complex models that represent the real application, which can be done by comparing simulated responses against experimental responses for such applications. In **Paper III**, a series of experiments were performed on a real hydraulic hammer product where measurements of typical variables were carried out. Further, a model which replicate the experimental setup was created using the co-simulation tool, and the responses from the experiments and the simulations were compared. In this chapter, a summary of this study is given while the complete study is presented in **Paper III**.

The dynamic sealing gaps implemented in the co-simulation tool, were verified in **Paper IV** using a model that represents the percussion unit. Four typical running conditions for the percussion unit were used to evaluate the implemented functions.

The wear behaviour in percussion units, which is presented in **Paper V**, was investigated by an experiment to find the tolerance against seizure, which is a severe type of wear damage. The hydraulic hammer was operated using a similar experimental setup as in **Paper III**, but the operating pressure was successively increased and the level of wear was registered at each step, until seizure occurred. A simulation model representing the experimental setup was developed using the co-simulation tool, and wear was simulated using the wear routines in LS-DYNA.

4.1 Experiments

To validate the functionality of the co-simulation tool a hydraulic hammer was set up in the in-house test rig, see Fig. 12, where it could be operated under steady and controlled conditions. The mechanical interfaces are the top plate, where the feeding force is applied, and at the bottom the anvil, where the tool is positioned to represent the working material. Hydraulic power is supplied to the hammer by an external power pack which allows for a wide range of different running conditions in terms of hydraulic pressure and flow. The hammer used in the experiments was an Epiroc SB202, see Fig. 2b, which is a 200 kg hydraulic hammer intended for, e.g., demolishing, trenching and mining work. The parts of the hammer and its working principle are described in Chapter 2. To register

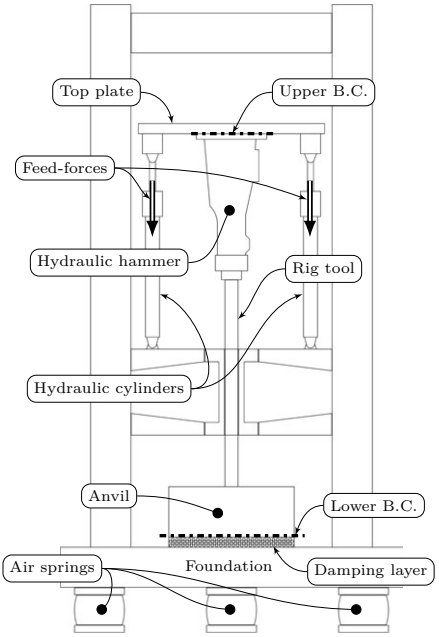

Figure 12: Schematic presentation of the test rig and the measurement setup. Figure from **Paper III**.

the working behaviour of the hammer a number of different type of sensors were used, such as position, accelerometer, strain and hydraulic pressure, see Fig. 13. Four different running conditions were identified, see Table 2, with the objective to investigate the variations in the responses from different parameter sets, and experimental data were collected for all four conditions.

The tolerance against seizure between the piston and the liner in the percussion unit was investigated by a second experiment where the same setup as in the previous experiment was used. The piston and the liner were replaced in the hydraulic hammer from the first experiment with components that were manufactured to achieve a specific clearance in between. The operating pressure was increased

Table 2: The four running conditions used in the experiments, and the diameter D_R of the Restrictor orifice. Table from **Paper III**.

	Operating pressure (Bar)	Oil flow (l/min)	$\varnothing D_R$ (mm)
Case 11	150	80	6.0
Case 12	150	66	5.4
Case 21	100	59	6.0
Case 22	100	50	5.4

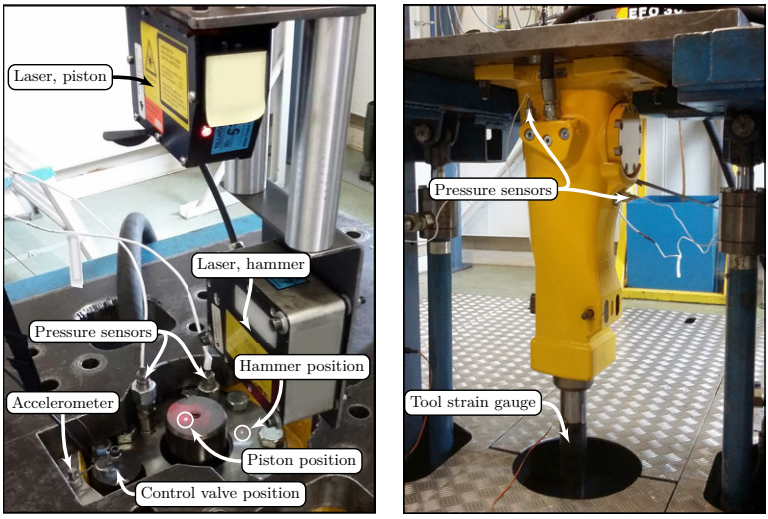

(a) **(b)**

Figure 13: The sensors on the upper side (a) and the sensors on the left side of the hammer (b). Figure from **Paper III**.

stepwise, and as the pressure increases, the pressure induced deformation of the liner will also increase, eventually the deformation will be larger than the actual clearance and contact between the piston and the liner will occur, thus generating wear. At each step, the hammer was disassembled and the wear damages on the piston and the liner were documented by photographs. When seizure could be confirmed the experiment was stopped, which happened after five steps at running condition 5. The running conditions and the results from the second experiment are presented in Table 3, where all values are normalised with respect to the running condition 5. In Table 3, the parameter $\overline{p}_{\mathrm{C}}$ refers to the average value of the operating pressure for the complete running cycle during the respective sequence, and the parameter Max Δp refers to the maximum difference between the pressure on the outside and on the inside of the liner.

Table 3: Normalised parameters and wear results from the second experiment. Table from **Paper V**.

Running condition	$\overline{p}_{\mathrm{C}}$ (-)	Max Δp (-)	Result
1	0.69	0.69	No wear
2	0.78	0.80	No wear
3	0.89	0.91	Polished
4	0.92	0.91	Polished
5	1.0	1.0	Seizure

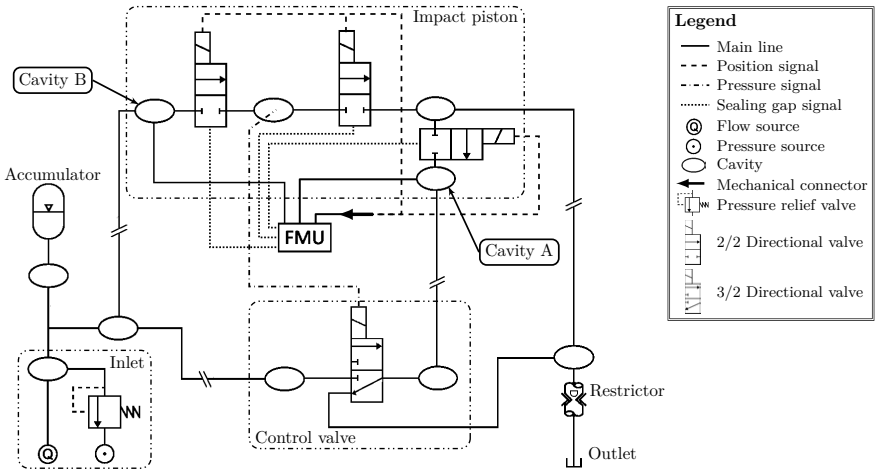

Figure 14: A schematic figure of the second fluid simulation model. The components belonging to each of the main functions are encircled: pressure inlet, impact piston and control valve. The restrictor is used to control the oil flow through the percussion unit. Figure from **Paper IV**.

4.2 Simulation models

Two simulation models were developed using the co-simulation tool described in Chapter 3, where the first model represents the experimental setup used to validate the functionality of the co-simulation tool in **Paper III**. The second model was first used to verify the functionalities of the dynamic sealing gaps in **Paper IV** and then to replicate the second experiment with the purpose to simulate wear in **Paper V**.

Two 1D models which represents the fluid system of the hydraulic hammer were developed using Hopsan, where the co-simulation interface was included as an FMU sub-component. Two 3D FE-models representing the structural parts of the hydraulic hammer were developed using LS-DYNA, which is described in Section 4.2.1. The fluid system models are complex networks of various types of sub-components such as channels, cavities, valves etc., which represent different features in the system. A schematic figure of the second fluid system model is presented in Fig. 14. The majority of the sub-components were standard components from the Hopsan libraries, but in-house developed components for an improved representation of the real mechanisms were also used.

In the first model, co-simulation was set up for the piston and the control valve to achieve an accurate representation of the mechanisms for these components, while only the piston was set up for co-simulation in the second model. In the second model, the control valve was represented by numerous 1D sub-components in the fluid system model. Furthermore, the motions of the housing, the valve cover and the rig tool were communicated to the fluid simulation model, and were used to control the valve components during the simulation. The valve components were

used to simulate the sealing gap mechanism in the percussion unit, where constant values for the gap height and eccentricity were used in the first model, while fully dynamic values were enabled in the second model.

4.2.1 Finite element models

The first FE-model represents the structural parts of the hydraulic hammer, the rig tool and the anvil, see Fig. 15, while the test rig was represented by discrete masses, spring and damper elements at the upper and lower boundary. The properties of the spring and damper elements were tuned to fit the experimental response of the housing motion as close as possible. Discrete mass elements were evenly distributed over the adapter plane on the housing to represent the mass of the test rig. Because the geometry of the hydraulic hammer is almost perfectly symmetric it was represented by a half model, and the corresponding boundary conditions, to reduce the computational resources and the time spent for each simulation.

Contact were defined for the parts which experience mechanical interactions to represent the real behaviour. In those where oil and grease are present at the contact surfaces the damping value was increased, from 10% to 50% of the critical viscous damping value.

The control valve is an internal part of the hydraulic hammer and is completely surrounded by oil, hence viscous forces will be generated when it moves through the fluid. These forces will be of particular importance at the mechanical end points,

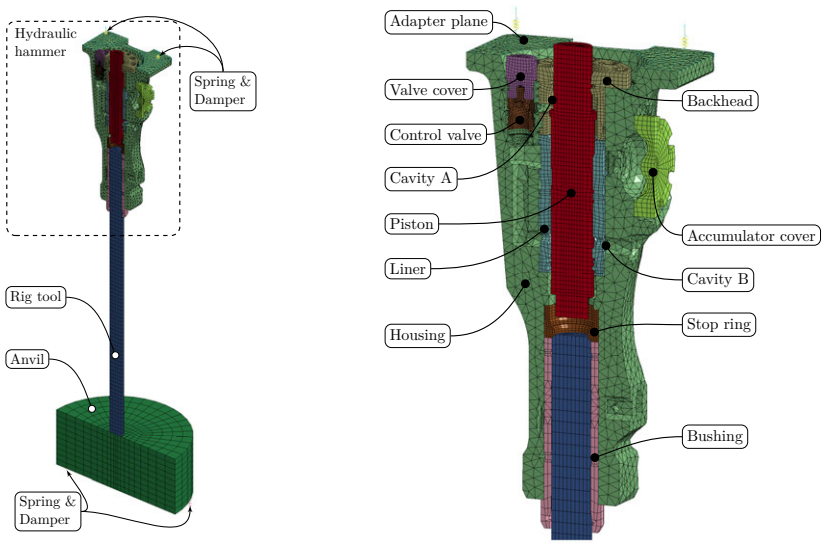

Figure 15: The (a) first FE-model used in **Paper III** and (b) its details.

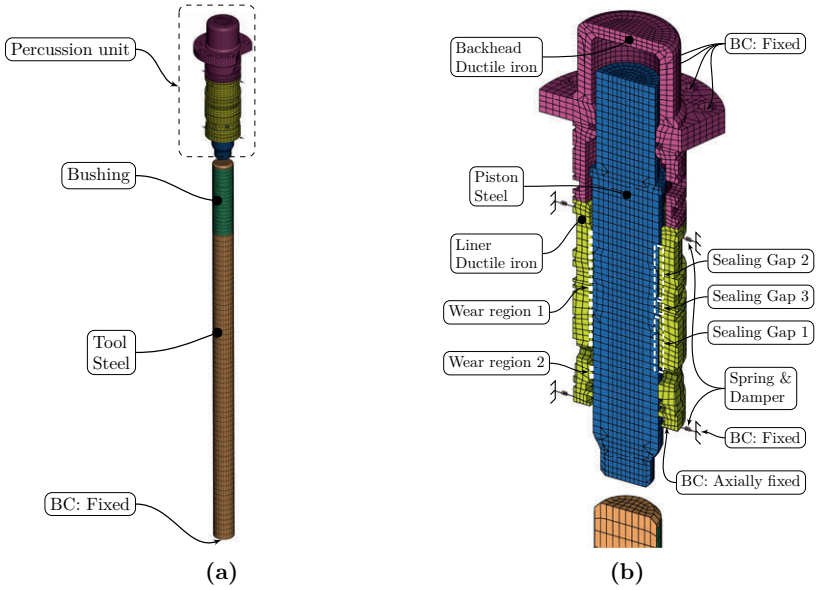

Figure 16: The (a) second FE-model used in **Paper IV** and **V** and (b) its details.

where the viscous forces, which is generated by compression of the fluid, will reduce the speed of the valve before it reaches its end point. This effect was realised by a routine in LS-DYNA that calculates a damping force that reduce the speed of the control valve before contact occur at the end points, see **Paper III** for more information of this routine. This was considered to be a practical approach because the oil film functionalities in the Mortar contact was not implemented in the R9.3 version of LS-DYNA that was used in this case.

The fluid loads were simulated in Hopsan and sent to the structural simulation using the co-simulation interface, where it were applied as pressures to the segments belonging to each of the cavities for the piston and the control valve. A control routine in LS-DYNA keeps track of which segment is inside or outside the cavity. When a segment moves outside the cavity the pressure is removed, and when the segment moves back inside, the pressure is restored. The friction force from the hydraulic sealings on the piston was simulated by Hopsan and transferred to LS-DYNA over the mechanical port for the piston. The feed-force on the hammer was simulated by a compressive prescribed displacement of the spring elements, which generates a compressive force on the structure.

The second FE-model used in this work is displayed in Fig. 16 and comprises the core components of the percussion unit according to Fig. 16b, all details regarding the model are presented in **Paper IV** and **V**.

The housing and the test rig were represented by the boundary conditions and the spring and damper elements, which properties were tuned to, by experience,

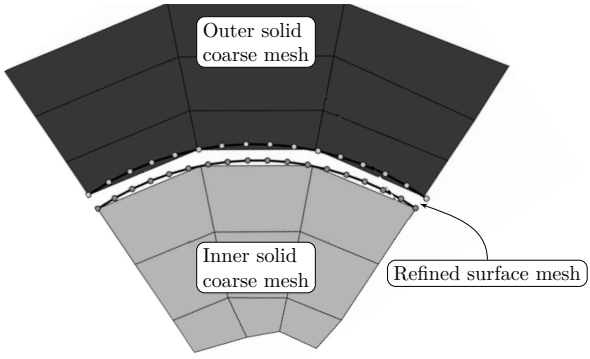

Figure 17: The refined surface mesh that creates a smooth description of the cylindrical surface.

give a realistic response of the liner. The feeding force of the hammer was not included in this model. The contact between the piston and the liner was modelled by two pairs of contacts using the Mortar contact routine in LS-DYNA, where one pair was representing the mechanical contact and the other the oil film mechanism according to Section 3.4. For the mechanical contacts the CONTACT_ADD_WEAR keyword were specified to call on the routines for simulating wear, where two regions of the model were defined, see Fig. 16. To improve the simulation of the contact, the method proposed by Haufe et al. [50] was used. In this method, a fine shell mesh is added on top of a coarse solid element mesh to which it is rigidly connected to transfer the contact forces between the different meshes, see Fig. 17. Hence, an accurate and smooth representation of the contact surface is achieved without the need to increase the number of solid elements. Co-simulation of three sealing gaps, see Fig. 16, was set up using the UDF keywords in LS-DYNA to invoke the routine for calculating the gap height and the eccentricity for each gap, which were relayed to the fluid system simulation for calculating the leakage flow.

4.2.2 Time step and mass scaling

Due to the implementation of the co-simulation interface a fixed time step of 2.7×10^{-7} s was used in both Hopsan and LS-DYNA. This time step size was determined from the smallest FE-element in the piston and the relevant Courant condition [47]. However, this choice of time step resulted in a minor mass scaling in some of the parts in the FE-model using the conventional mass scaling in LS-DYNA, which is also discussed in **Paper III**. Components from fluid power machinery tend to have narrow sections that generates small elements when modelled by finite elements, and thus generating small time steps. If small time steps are used without mass scaling, the time spent on the simulation may increase drastically. Furthermore, it is important to monitor the effects of the mass scaling because it can significantly affect the dynamic properties of the body, and for components

with large rigid body movement the mass scaling should be reduced to a minimum. In this study, a mass scaling of 1.8% and 5.8% for a component with large and negligible rigid body movements respectively were found to be acceptable for this application.

4.2.3 Execution

The fluid simulation models were initialised by the starting positions for all mechanical components, which were related to the corresponding positions in the FE-models, and, further the initial speed was set to zero for all components. The initial pressure on the high pressure side was set to 15 MPa and to 100 kPa on the low pressure side. The pre-loaded stress state, which simulate the feeding force on the hammer, of the first FE-model was initialised by use of the explicit dynamic relaxation routine in LS-DYNA. This step was excluded for the second model because no feed-force was active. At the start of the simulation, the flow source delivers a constant oil flow to the percussion unit, and as the simulation advances the pressure will increase and eventually the piston and the control valve will start to move. The operating pressure was controlled by the pressure relief valve at the inlet side, see Fig. 14. A steady state behaviour was reached for the piston motion after a few working cycles, and transients from the start-up phase had faded out. The running conditions were realised in the simulations by changing the inlet pressure and the orifice diameter of the restrictor in the fluid simulation models. Five to six complete working cycles were simulated, which represented a total time of 0.3–0.4 s.

4.3 Outcome

Considering that the experiments were done to validate the co-simulation tool rather than investigating the absolute behaviour of the hydraulic hammer, all simulated responses were normalised against the corresponding experimental results. To reveal the basic characteristic of the signals these were low pass filtered at 500 Hz, and this was done for both the experimental and the simulated signals, except for the rig tool stress. Furthermore, certain important operating parameters for the hydraulic hammer were calculated using the time domain signals, e.g., the stroke length and the impact frequency were estimated from the piston position. The impact energy is one of the most important property of a percussion unit, and this property was estimated from the primary stress wave in the tool, see for instance Lundberg [51]. The impact energy W was calculated according to the following equation

$$W = \frac{A\, c_0}{E_{\text{Steel}}} \int_{t_1}^{t_2} \sigma_{\text{Tool}}^2 dt, \tag{19}$$

where A is the cross section area of the rig tool, c_0 is the speed of sound in the material and is calculated as

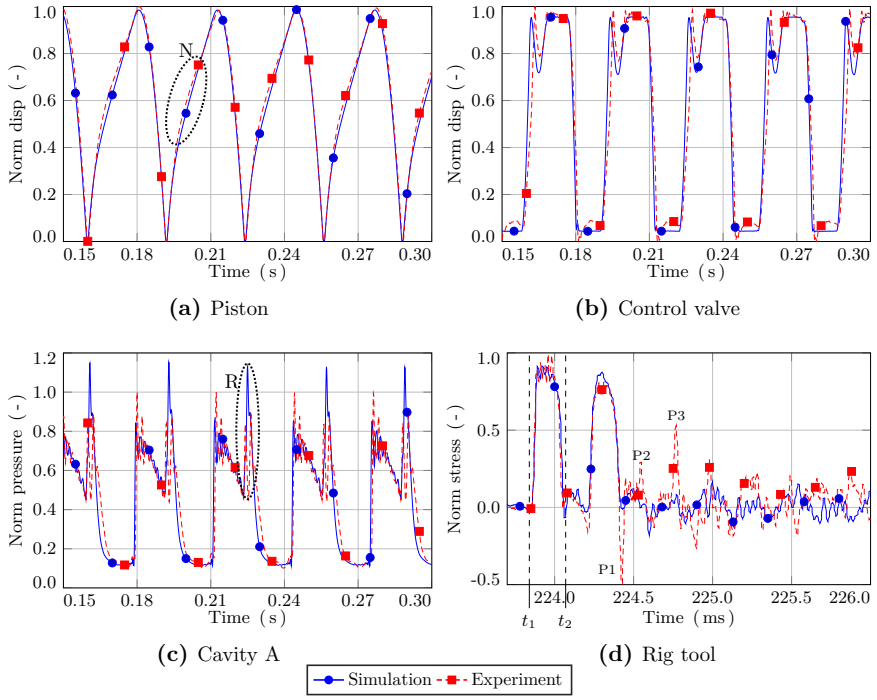

(a) Piston **(b)** Control valve

(c) Cavity A **(d)** Rig tool

Figure 18: Simulation and experimental results from Case 11. Marked regions or events of the signals, i.e. region N in (a) and region R in (c), where deviations or typical behaviour have been noticed. In (d), the integration limits t_1 and t_2 used in the calculation of the impact energy are displayed. Redrawn from **Paper III**.

$$c_0 = \sqrt{\frac{E_{\text{Steel}}}{\rho_{\text{Steel}}}} \tag{20}$$

and the integration limits are shown in Fig. 18d, i.e. t_1 and t_2. E_{Steel} and ρ_{Steel} are the elastic modulus and the density of the steel material in the rig tool, respectively. As an example, four responses from the running condition Case 11 are shown in Fig. 18, together with the corresponding experimental responses.

In general a very good agreement to the experiments was found by using the developed co-simulation approach. The simulated responses of the piston and the control valve are very similar to the experiments, see Fig. 18, where the curves are almost identical, which suggest that the simulation model to a large extent represents the real mechanisms in the hammer. The orifice diameter of the restrictor in the simulation model was tuned to meet the impact frequency in Case 11 from

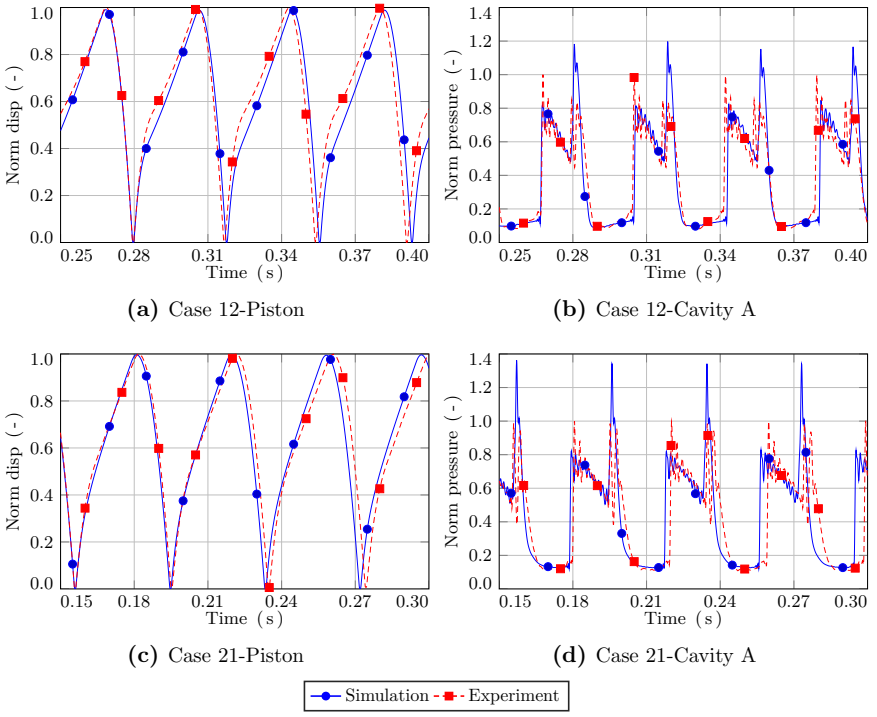

(a) Case 12-Piston **(b)** Case 12-Cavity A

(c) Case 21-Piston **(d)** Case 21-Cavity A

Figure 19: Comparison of results from the simulations and experiments. Showing the piston position for (a) Case 12 and (c) Case 21 respectively, and (b) and (d) the pressure in cavity A for the corresponding running conditions. Redrawn from **Paper III**.

the experiment, and this can also be observed in Fig. 18, where the point of impact is exactly the same. However, some minor deviations could be noticed, see region N and R in Fig. 18, which can be related to the modelling of the fluid system and the boundary conditions of the FE-model, see **Paper III**. Furthermore, the responses of the pressure and the stress confirm that the model also is capable to represent the essential mechanisms of wave propagation in the fluid system and the structure. The results from the other running conditions, i.e. Case 12, 21 and 22, confirms the same behaviour as for Case 11 for the piston position and the pressure in Cavity A, where the results from Case 12 and 22 are presented in Fig. 19. Normalised average values from all running conditions are presented in Table 4, see **Paper III** for the details of the calculation of these values.

Table 4: Normalised values from the simulations with respect to the experiments, presented as percentage values. Data from **Paper III**.

	Case 11	Case 12	Case 21	Case 22
Norm W	97.3	95.3	95.3	96.6
Norm f	100.1	98.4	101.9	101.3
Norm Δu_{p}	99.2	99.3	99.6	99.8
Norm Q_{In}	105.3	108.8	114.9	117.3
Norm p_{In}	99.6	100.2	100.2	99.9
Norm p_{Out}	132.1	95.0	101.0	78.0
Norm p_{A}	100.3	100.0	106.7	106.2
Norm p_{B}	98.8	99.5	99.4	99.3
Norm σ_{Tool}	98.1	95.2	99.8	100.4

The functions and routines that were implemented in the simulation tool to facilitate simulation of dynamic sealing gaps, see Section 3.3, were verified by simulations using the second model that is described in Section 4.2. The fluid system was simulated using the model, which schematically is shown in Fig. 14, and the FE-model of the structural parts are shown in Fig. 16. Three sealing gaps were set up for co-simulation and the oil film between the piston and the liner was modelled using the approach described in Section 3.4. Four running conditions for the percussion unit were defined to verify the behaviour of the sealing gaps, which are presented in Table 5. In Case I and II, constant values for the calculation of the leakage flow in the simulation were used, which is the same approach as in **Paper III**, while all functionalities of the sealing gap simulation were enabled in Case III and IV. In Case IV, a misaligned impact was simulated, see Fig. 20, which refers to a small misalignment of the tool during the impact that will induce radial motions of the piston and by that eccentric annuluses may be formed for the sealing gaps. This behaviour will affect the calculation of the leakage flow through the sealing gap when it is closed. Some results from the simulations are presented in Fig. 21, showing the ratio of the clearance, the eccentricity and the

Table 5: Running conditions used when verifying the sealing gap simulations. Table from **Paper IV**.

Case	Title	Gap height	Eccentricity	Angle of impact
I	Constant	Constant	Constant Zero	Straight
II	Eccentric	Constant	Constant Max	Straight
III	Straight	Dynamic	Dynamic	Straight
IV	Misaligned	Dynamic	Dynamic	Misaligned

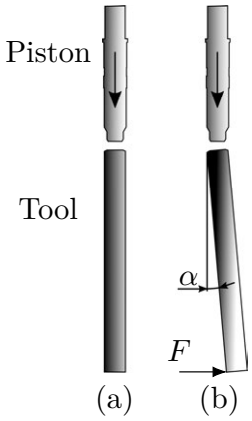

Figure 20: Different type of impacts, (a) the normal straight impact and (b) the misaligned impact, where the tool is inclined an angle of α. The external force F pushes the tool to the misaligned position. Figure from **Paper V**.

normalised leakage flow. The normalised clearance for Case I and II is equal to one, and the eccentricity ratio is equal to zero for Case I and equal to one for Case II. For Case III and IV these variables varies due to pressure induced deformations and radial motions of the liner and the piston due to the misaligned impact, and these responses are affecting the leakage flow through the closed sealing gap. The eccentricity values for Gap 1 and 2 are high at the time of impact but they fade out quite rapidly, which is an effect of the oil film that will force the piston to a concentric position. This effect cannot be noticed for Gap 3 because the position of this gap is placed near the rotational centre of the piston, in the lengthwise direction, and will not experience any large radial motions. Another variable which also has a significant influence on the leakage flow is the gap length, which is further discussed in **Paper IV**.

Wear was simulated in the percussion unit by the second simulation model, which is described in Section 4.2, and it was set up to replicate the second experiment, see Section 4.1, where the wear in the unit was investigated. The operating pressure and the impact frequency in the simulations were tuned to fit the experimental responses with the intention to reduce the number of uncertainties in the evaluation of wear. Two regions for simulation of wear were defined according to the method described in Section 3.5. Wear patterns from the experiment and the simulations are shown in Fig. 22. Five steps until seizure occurred were required, where no wear could be observed for running condition 1 and 2, while a low degree of wear were registered for running condition 3 and 4, see Fig. 22a and b, and the seizure damages at running condition 5 are presented in Fig. 22c.

The wear from a misaligned impact was also simulated, see Fig. 23, which must be considered as quite common for a hydraulic hammer in real work, and therefore it is of great importance that it is possible to simulate such running conditions.

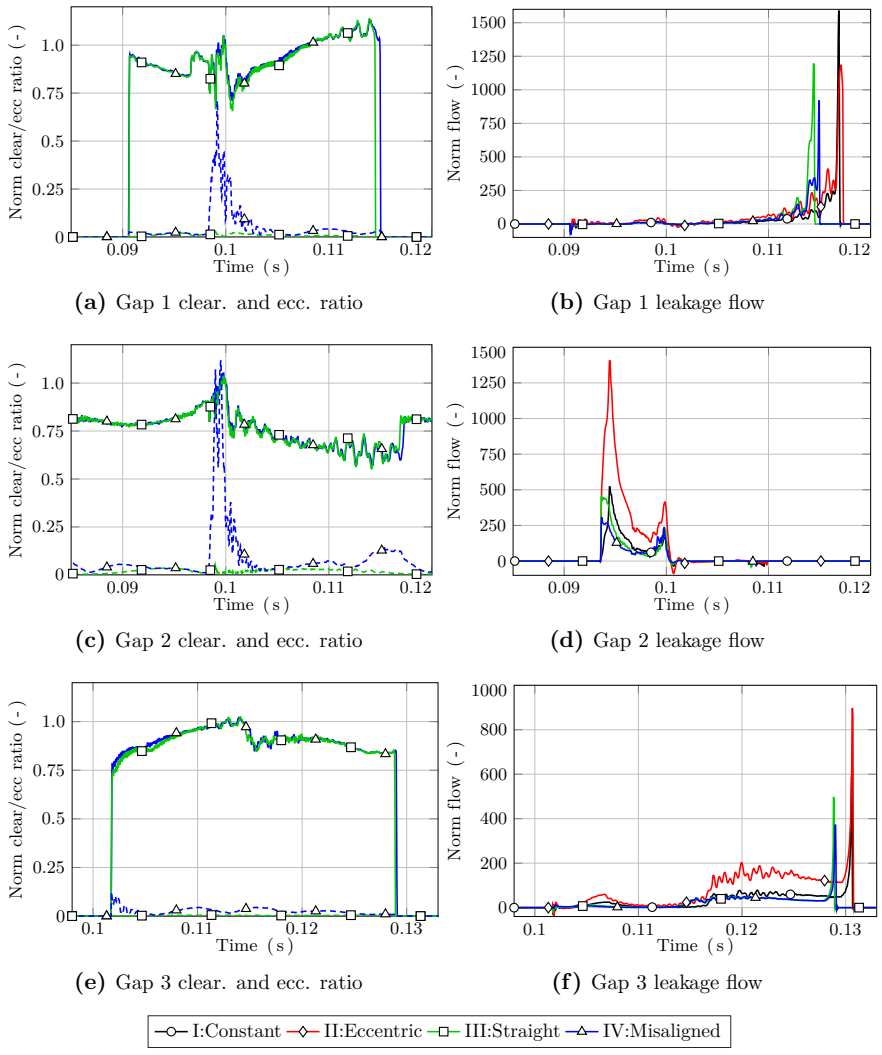

(a) Gap 1 clear. and ecc. ratio

(b) Gap 1 leakage flow

(c) Gap 2 clear. and ecc. ratio

(d) Gap 2 leakage flow

(e) Gap 3 clear. and ecc. ratio

(f) Gap 3 leakage flow

Figure 21: Results from the simulations where dynamic sealing gaps are utilised. In (a), (c) and (e) the solid lines represent the clearance and the dashed lines the eccentricity ratio for Case III and IV. Redrawn from **Paper IV**.

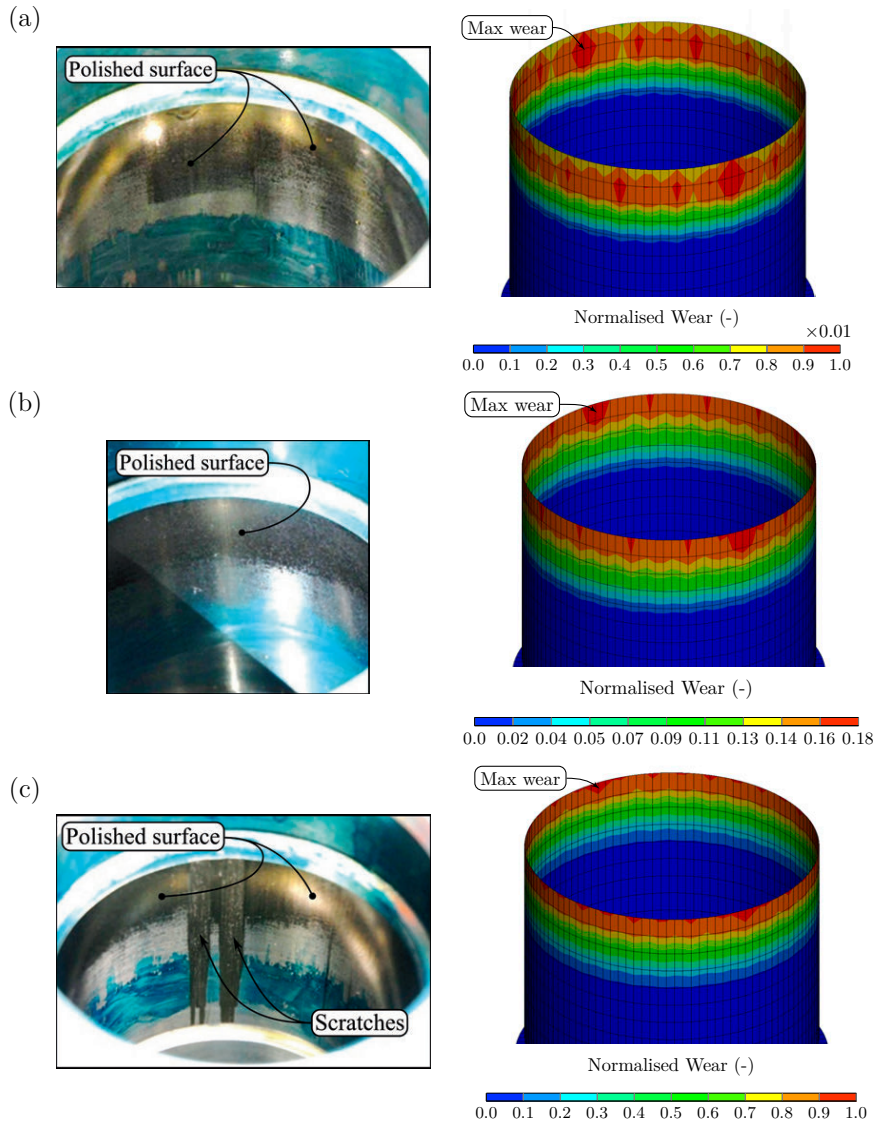

Figure 22: Wear patterns on the liner from the experiment and the simulations for the cases where wear occurred. The operating condition where seizure occurred (c) and the conditions where a lower degree of wear were observed (a) and (b). Figure from **Paper V**.

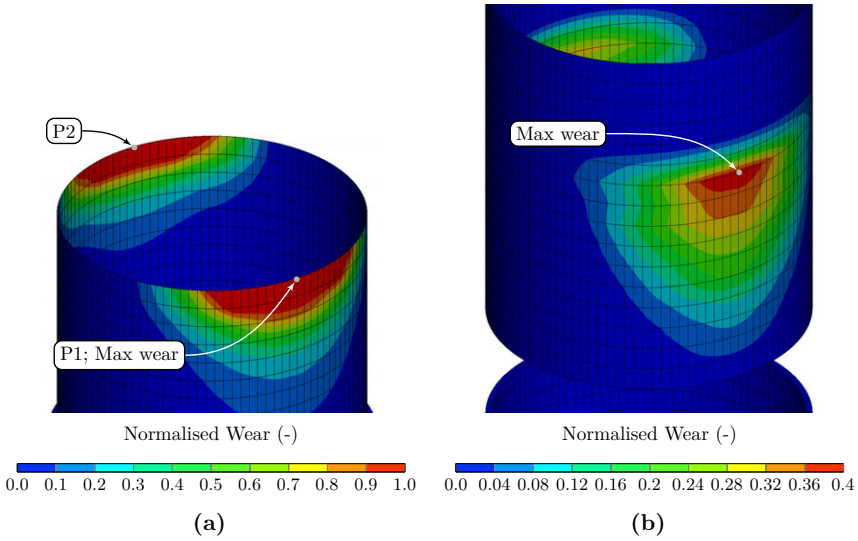

Figure 23: Wear patterns from the simulation of a misaligned impact on (a) the liner and (b) the piston. Redrawn from **Paper V**.

4.4 Parameter study

To investigate the response from the first simulation model when changing the value of an input parameter, hence a parameter study was performed. The following parameters were included in the study: the operating pressure, as the time average value of the input pressure, $\overline{p}_{\text{In}}$, and the orifice diameter, D_R, of the restrictor, which affects the input flow, $\overline{Q}_{\text{In}}$, and the impact frequency, $\overline{f}$. The responses evaluated were input and output power, P_{Input} and P_{Output} respectively, that were calculated as follows

$$P_{\text{Input}} = \overline{p}_{\text{In}}\, \overline{Q}_{\text{In}}\ , \tag{21}$$

$$P_{\text{Output}} = \overline{W}\, \overline{f}\ . \tag{22}$$

Furthermore, the calculated values of power were normalised to emphasise the relative differences of the results. A normalisation with respect to Case 11 was carried out according to the following equations

$$\text{Norm } P_{\text{Input}} = \frac{P_{\text{Input}_n}}{P_{\text{Input}_{11}}}, \tag{23}$$

$$\text{Norm } P_{\text{Output}} = \frac{P_{\text{Output}_n}}{P_{\text{Output}_{11}}}, \tag{24}$$

where the index n represent the running conditions Case 12, Case 21 and Case 22. Figure 24 display the normalised values of the input and output power. The responses of the simulation model from the parameter changes represents the corresponding experimental results to a large extent. Hence, a good prediction of the response of a parameter change of the model can be expected by using the co-simulation tool.

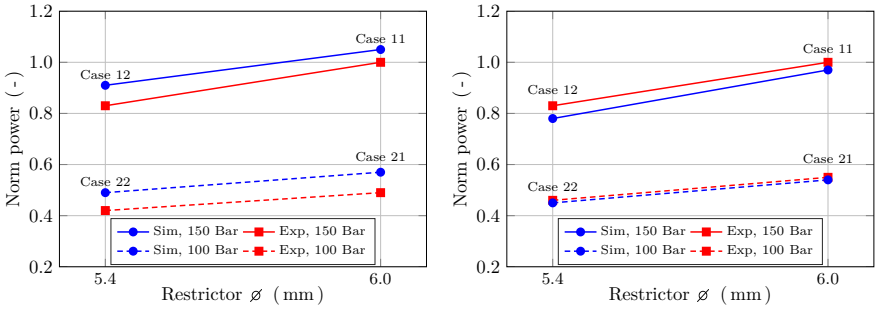

(a) Input power, $P_{\text{Norm Input}}$ **(b)** Output power, $P_{\text{Norm Output}}$

Figure 24: The results from the parameter study. Redrawn from **Paper III**.

5 Conclusions and outlook

5.1 Conclusions

The main objective has been reached by developing a co-simulation approach between a 1D fluid system and a 3D structural FE-model and it has been shown that it is possible to establish a communication procedure between these models. This approach facilitates an overall system evaluation of performance and efficiency, and the 3D FE-model enable evaluations of deformations and stresses. It has also been shown that it is possible to co-simulate several components, which is an important requirement because the percussion unit consists of several moving components. The responses for a hydraulic hammer have been simulated replicating the experimental setup and it has been shown that the real responses could be reproduced using the co-simulation tool.

To further enhance the prediction and to increase the simulation capabilities of the co-simulation tool, two additional objectives were defined: dynamic simulation of the sealing gap mechanism and simulation of wear. To achieve a dynamic simulation of the sealing gap mechanism a method was developed that parametrise the deformed structure of the sealing gap region, the parameters were then relayed to the fluid system simulation for calculation of the leakage flow. This method shows that it is possible to utilise the elastic deformations of the FE-model to enhance the simulation of the sealing gap mechanism. Finally, it has been shown that it is possible to simulate wear in percussion units using the co-simulation tool. To simulate wear, the responses of the percussion unit was first simulated by the use of the co-simulation tool and the wear routines in the FE-software were then utilised for calculation of wear. Table 6 presents an overview regarding the defined research questions and in which papers they are addressed.

Table 6: The papers and the research questions addressed.

RQ	**Paper I**	**Paper II**	**Paper III**	**Paper IV**	**Paper V**
1	X	X		X	
2		X	X	X	X
3			X		X
4				X	X
5					X

5.2 Outlook

Modelling of hydraulic percussion units involves the areas of fluid, solid mechanics and tribology, where the coupled fluid and structure mechanisms are of main importance. The co-simulation tool that has been developed in this project has shown to replicate the main and essential mechanisms to a large extent, and can be considered promising as an efficient tool for this application. In the course of this work, a few different issues have been identified which may be considered for further development of the co-simulation tool.

- To make the co-simulation tool even more versatile, a method for predicting the radiated noise from hydraulic hammers should be developed. The vibrations of the outer parts of the hammer are calculated by the structural simulation in the tool, and within LS-DYNA there are routines to calculate the radiated noise. Since these parts constitutes the baseline for noise predictions and is available today, it should be rather inexpensive to develop such a method.
- To simulate the fragmentation of concrete, which is the typical working material for the hydraulic hammer, is of great interest. Such method can, e.g., be used to study the overall productivity, from hydraulic input power to the volume of fragmented concrete, but it may also provide a more realistic boundary condition for the tool, for instance, when the radiated noise are to be studied.
- In this work the co-simulation tool has been implemented for Shared Memory Processing (SMP) for LS-DYNA, which do not scale as good as the Massively Parallel Processing (MPP) when increasing the number of processors. Development for support of MPP must be considered urgent, especially when the size and complexity of the models, and also the analysis times, tend to increase.
- The oil film that is formed between the piston and the liner is crucial when analysing the lateral behaviour of the percussion unit from, e.g., a misaligned impact. The modelling of the oil film is based on equations, which are derived from Reynolds equation, and are developed for squeeze film dampers for gas turbines. In the percussion unit the axial and radial motions are combined that might end up in a different behaviour for the oil film. State of the art today is to solve Reynolds equation and heat transfer simultaneous to calculate the fluid pressure in the oil film, which has, for instance, been done by Chacon and Ivantysynova [52]. Ultimately, the properties of the oil film should be experimentally validated.

- This task concerns the use of multiple FMUs. Today only one FMU is permitted in the system simulation model and all fluid structure couplings must be connected to this component. The complexity and size of the models are continuously increasing and the system simulation model tend to be quite unstructured, especially when multiple components are to be simulated. The use of multiple FMUs would facilitate a more structured system simulation model. However, the solution of this is not straight forward, since the communication to the FE-software must be synchronised for all FMUs.
- Cavitation is a mechanism that may cause significant damages in the percussion unit which has not been studied in this work. Cavitation induced damages are classified as an erosive wear where the solid material is removed by high short duration pressure peaks which are generated by collapsing bubbles in the fluid. The bubbles are mainly generated from a rapid pressure drop in the fluid, e.g., when closing a valve. The fluid simulation that is implemented in the co-simulation tool today facilitates studies of cavitation on a quite rough level and other methods are necessary for more comprehensive analyses of cavitation.

6 Review of appended papers

Paper I

A co-simulation method for system level simulation of fluid-structure couplings in fluid power systems

Review: A co-simulation method is presented for fluid power machinery, that is based on a 1D system simulation model representing the fluid system, and a 3D finite element model representing the structural components. The method was implemented using two well-known simulation tools, Hopsan and LS-DYNA, and a co-simulation interface was realised by the use of the Functional Mock-up Interface standard. The TLM technique is used in Hopsan for the fluid system simulation, and the related major issues were presented and discussed. On the LS-DYNA side, the co-simulation interface was implemented by the use of the User Defined Feature module. A simple fluid power model, where the main mechanisms for a hydraulic percussion unit are represented, was developed in order to verify the co-simulation approach against a reference model in the stand-alone version of Hopsan. The verification indicates that correct and stable results are obtained, and that the high frequency mechanisms, which are related to the wave propagation, are resolved. A final case was also analysed where the structural parts were modelled using linear elastic material properties, and also with relevant contacts, with the aim to demonstrate the potential of this method when full 3D FE-results are available from the simulation.

Paper II

System level co-simulation of a control valve and hydraulic cylinder circuit in a hydraulic percussion unit

Review: Further development of the previously proposed co-simulation tool was done to enable multiple fluid-structure couplings. In this study a more complex model was set up, in which two components were defined for co-simulation. This model, which include the couplings for both the main piston and the control valve, represents the real application to a further extent than the simple model of only one cylinder presented in **Paper I**. Two models were developed and evaluated, one simple using a rigid body representation, and one more complex where a linear

elastic representation of the structural components is utilised. The responses from the co-simulation model for the simple case were compared against the responses from a reference model in Hopsan, which resulted in good agreement but with a small time shift, which however can be considered negligible for this application. Typical mechanisms of short duration and high amplitude for the hydraulic percussion unit was found to compare well, and can properly be represented by the co-simulation method. The second case, using a linear-elastic representation of the structural parts, was meant as a demonstration of the method for an industrial application, closer to reality, and also here the high frequency mechanisms are well represented by the co-simulation method.

Paper III

Validation of a co-simulation approach for hydraulic percussion units applied to a hydraulic hammer

Review: In this paper the co-simulation tool has been utilised to simulate the responses of an existing hydraulic hammer product. In order to validate the simulation model, experiments were performed using four different running conditions. The simulation model was developed using the co-simulation tool, and the responses were simulated for the corresponding running conditions. The typical mechanisms in the hydraulic hammer generate high frequency and high amplitude excitations, which require a high resolution of the model dynamics from the simulation model. The comparison against experimental data successfully confirms that the simulation model represents the mechanisms in the hydraulic hammer with good agreement, not only on the overall level but also on the detailed component level. Further, a parameter study was performed to investigate the response from the simulation model when changing the operating pressure and the orifice diameter of the restrictor. The responses were then compared to the corresponding changes from the experiments. The study confirms a correct response from a design parameter change in the simulation model.

Paper IV

Simulation of leakage flow through dynamic sealing gaps in hydraulic percussion units using a co-simulation approach

Review: In this study, the co-simulation tool has been expanded to simulate the dynamic behaviour of the sealing gap in hydraulic percussion units. The sealing gap is essential for the fundamental functions of a percussion unit where it play several important roles. The internal pressure inside a fluid powered machine will deform the structure to a certain degree, and this in turn affects the sealing capability of the sealing gap at the closed phase. In this study, routines has been developed and implemented in LS-DYNA to parameterise the structural deformation of the

sealing gap region for the FE-model. The parameters represent the radial clearance and the eccentric position for an annular gap, and these are communicated to the fluid simulation to enhance the simulation of the leakage flow through the gap. The simulation results show that the leakage flow will decrease when using dynamic sealing gaps, mainly depending on the reduction of the clearances.

Paper V

Simulation of wear in hydraulic percussion units using a co-simulation approach

Review: A method to simulate wear by use of the co-simulation tool and the wear routines in LS-DYNA is presented. The effects of wear has a negative impact on performance and life for hydraulic percussion units and is today mainly evaluated on physical prototypes. Methods to perform model-based evaluations of wear would be of great help because test of physical prototypes is time consuming and require large resources. In this paper, one experiment has been performed to investigate the tolerance against seizure for a hydraulic percussion unit. In this experiment, the operating pressure was increased, stepwise, until seizure occurred, and the wear related damages were documented for each step. The co-simulation tool has been utilised to simulate the responses of a model representing the experimental setup and the wear was simulated by use of the wear routines in LS-DYNA. The wear patterns from the experiment and the simulations were found to correspond to a large extent. Furthermore, the wear from a misaligned impact was simulated with the intention to demonstrate the capability of this method.

Bibliography

[1] L. L. Lysenko and L. V. Gorodilov, "Optimizing pulsed-machine parameters.," *Journal of Mining Science*, vol. 33, no. 4, p. 356, 1997.

[2] L. V. Gorodilov, "Calculation of the main parameters of a hydraulic percussive machine.," *Journal of Mining Science*, vol. 35, no. 2, p. 177, 1999.

[3] L. V. Gorodilov, "Analysis of working cycle of hydraulic impact machine using similarity criteria.," *Journal of Mining Science*, vol. 36, no. 5, p. 476, 2000.

[4] L. V. Gorodilov, "Investigation into characteristics of working cycles of hydraulic percussive machines with ideal distributor.," *Journal of Mining Science*, vol. 38, no. 1, p. 74, 2002.

[5] L. V. Gorodilov, "Mathematical models of hydraulic percussion systems," *Journal of Mining Science*, vol. 41, pp. 475–489, Sep 2005.

[6] L. V. Gorodilov, "Numerical study into dynamics of self-oscillatory hydropercussion systems. part I: Double-acting systems.," *Journal of Mining Science*, vol. 43, no. 6, pp. 625–639, 2007.

[7] L. V. Gorodilov, V. G. Kudryavtsev, and O. A. Pashina, "Experimental research stand and procedure for hydraulic percussion systems.," *Journal of Mining Science*, vol. 47, no. 6, pp. 778–786, 2011.

[8] L. V. Gorodilov, V. P. Efimov, and V. G. Kudryavtsev, "Modeling the striking head-impact tool-rock mass interaction.," *Journal of Mining Science*, vol. 49, no. 4, pp. 618–624, 2013.

[9] Siemens PLM Software Simcenter, "Simcenter Amesim," 2021. (visited on 1/12/2021).

[10] A. Giuffrida and D. Laforgia, "Modelling and simulation of a hydraulic breaker," *International Journal of Fluid Power*, vol. 6, no. 2, pp. 47–56, 2005.

[11] A. Ficarella, A. Giuffrida, and D. Laforgia, "Numerical investigations on the working cycle of a hydraulic breaker: Off-design performance and influence of design parameters," *International Journal of Fluid Power*, vol. 7, no. 3, pp. 41–50, 2006.

[12] A. Ficarella, A. Giuffrida, and D. Laforgia, "Investigation on the impact energy of a hydraulic breaker," Tech. Rep. 2007-01-4229, SAE Technical Paper, 2007.

[13] A. Ficarella, A. Giuffrida, and D. Laforgia, "The effects of distributor and striking mass on the performance of a hydraulic impact machine," in *Commercial Vehicle Engineering Congress & Exhibition*, SAE International, oct 2008.

[14] J.-Y. Oh, G.-H. Lee, H.-S. Kang, and C.-S. Song, "Modeling and performance analysis of rock drill drifters for rock stiffness," *International Journal of Precision Engineering and Manufacturing*, vol. 13, pp. 2187–2193, Dec 2012.

[15] ANSYS. Inc, *ANSYS 2022 R1 Mechanical User's Guide*. Canonsburg, Pennsylvania, USA, 2022.

[16] LST, *LS-DYNA R12 Keyword User's Manual*. Livermore Software Technology, Livermore, USA, 2020.

[17] F. Casadei, J. Halleux, A. Sala, and F. Chillè, "Transient fluid-structure interaction algorithms for large industrial applications," *Computer Methods in Applied Mechanics and Engineering*, vol. 190, no. 24–25, pp. 3081–3110, 2001.

[18] Y. Wang, J. Feng, B. Zhang, and X. Peng, "Modeling the valve dynamics in a reciprocating compressor based on two-dimensional computational fluid dynamic numerical simulation," *Proceedings of the Institution of Mechanical Engineers, Part E: Journal of Process Mechanical Engineering*, vol. 227, no. 4, pp. 295–308, 2013.

[19] P. Krus, A. Jansson, J.-O. Palmberg, and K. Weddfelt, "Distributed simulation of hydromechanical systems," in *The Third Bath International Fluid Power Workshop*, (Bath, England), 1990.

[20] K. Stavåker, S. Ronnås, M. Wlotzka, V. Heuveline, and P. Fritzson, "PDE modeling with Modelica via FMI import of HiFlow3 C++ components," in *Proceedings of SIMS 54th Conference on Simulation and Modelling*, (Bergen, Norway), pp. 16–23, 2013.

[21] M. Ljubijankic, C. Nytsch-Geusen, J. Rädler, and M. Löffler, "Numerical coupling of Modelica and CFD for building energy supply systems," in *Proceedings of the 8th International Modelica Conference*, vol. 2011, (Dresden, Germany), pp. 286–294, Citeseer, March 2011.

[22] R. Kossel, W. Tegethoff, M. Bodmann, and N. Lemke, "Simulation of complex systems using Modelica and tool coupling," in *5th Modelica Conference*, vol. 2, pp. 485–490, September 2006.

[23] D. Z. Wu, Q. L. Liu, P. Wu, L. Q. Wang, T. Paulus, B. G. Wang, and M. Oesterle, "The research of 1D/3D coupling simulation on pump and pipe

system," *IOP Conference Series: Earth and Environmental Science, 26th IAHR Symposium on Hydraulic Machinery and Systems*, vol. 15, no. 5, 2012.

[24] G. Rauch, J. Lutz, M. Werner, S. Gurwara, and P. Steinberg, "Synergetic 1D-3D-coupling in engine development part i: Verification of concept," tech. rep., SAE Technical Paper, 2015.

[25] P. Bayrasy, M. Burger, C. Dehning, I. Kalmykov, and M. Speckert, "Applications for MBS-FEM-coupling with MpCCI using automotive simulation as example," in *Proceedings of the 2nd Commercial Vehicle Technology Symposium (CVT 2012)*, (Kaiserslautern, Germany), pp. 385–394, March 2012.

[26] H. Anzt, W. Augustin, M. Baumann, H. Bockelmann, T. Gengenbach, T. Hahn, V. Heuveline, E. Ketelaer, D. Lukarski, A. Otzen, S. Ritterbusch, B. Rocker, S. Ronnas, M. Schick, C. Subramanian, J.-P. Weiss, and F. Wilhelm, "Hiflow3 – a flexible and hardware-aware parallel finite element package," *Preprint Series of the Engineering Mathematics and Computing Lab*, vol. 0, no. 06, 2010.

[27] H. Andersson, *A Co-Simulation Approach for Hydraulic Percussion Units*. Licentiate thesis, Linköping University, Solid Mechanics, Faculty of Science & Engineering, 2018.

[28] T. Blochwitz, M. Otter, J. Åkesson, M. Arnold, C. Clauss, H. Elmqvist, M. Friedrich, A. Junghanns, J. Mauss, D. Neumerkel, H. Olsson, and A. Viel, "Functional mockup interface 2.0: The standard for tool independent exchange of simulation models," in *Proceedings of the 9th International Modelica Conference*, (Munich, Germany), pp. 173–184, September 2012.

[29] A. Kleist, "Design of hydrostatic bearing and sealing gaps in hydraulic machines– a new simulation tool," in *Fifth Scandinavian International Conference on Fluid Power. SICFP*, vol. 97, pp. 157–169, 1997.

[30] J. Bergada, S. Kumar, D. L. Davies, and J. Watton, "A complete analysis of axial piston pump leakage and output flow ripples," *Applied Mathematical Modelling*, vol. 36, no. 4, pp. 1731–1751, 2012.

[31] M. Ivantysynova, "A new approach to the design of sealing and bearing gaps of displacement machines," in *Proceedings of the JFPS International Symposium on Fluid Power*, vol. 1999 of *4*, pp. 45–50, The Japan Fluid Power System Society, 1999.

[32] M. Ivantysynova and C. Huang, "Investigation of the gap flow in displacement machines considering elastohydrodynamic effect," in *Proceedings of the JFPS International Symposium on Fluid Power*, vol. 2002 of *5-1*, pp. 219–229, The Japan Fluid Power System Society, 2002.

[33] M. Ivantysynova and R. Lasaar, "An investigation into micro-and macrogeometric design of piston/cylinder assembly of swash plate machines," *International Journal of Fluid Power*, vol. 5, no. 1, pp. 23–36, 2004.

[34] P. Agarwal, A. Vacca, K. Wang, K. S. Kim, and T. Kim, "An analysis of lubricating gap flow in radial piston machines," *SAE International Journal of Commercial Vehicles*, vol. 7, no. 2014-01-2407, pp. 524–534, 2014.

[35] B. Kamaraj, S. C. Subramanian, and B. Rakkiappan, "Numerical analysis of fluid-fluid interaction and flow through micro clearance to estimate leakages in a fuel injection pump," in *ASME 2014 International Mechanical Engineering Congress and Exposition*, vol. Volume 7: Fluids Engineering Systems and Technologies, American Society of Mechanical Engineers Digital Collection, 2014.

[36] B. Kamaraj, S. C. Subramanian, and B. Rakkiappan, "Numerical and experimental analysis of fluid–fluid interaction and flow through micro clearance to estimate leakages in a fuel injection pump," *Proceedings of the Institution of Mechanical Engineers, Part C: Journal of Mechanical Engineering Science*, vol. 231, no. 11, pp. 2054–2065, 2017.

[37] D. Thiagarajan and A. Vacca, "Mixed lubrication effects in the lateral lubricating interfaces of external gear machines: Modelling and experimental validation," *Energies*, vol. 10, no. 1, p. 111, 2017.

[38] N. Ohmae and T. Tsukizoe, "Analysis of a wear process using the finite element method," *Wear*, vol. 61, no. 2, pp. 333–339, 1980.

[39] P. Põdra and S. Andersson, "Simulating sliding wear with finite element method," *Tribology international*, vol. 32, no. 2, pp. 71–81, 1999.

[40] J. Archard, "Contact and rubbing of flat surfaces," *Journal of applied physics*, vol. 24, no. 8, pp. 981–988, 1953.

[41] T. Borrvall, A. Jernberg, M. Schill, L. Deng, and M. Oldenburg, "Simulation of wear processes in LS-DYNA," in *14th International LS-DYNA Users Conference, June 12-14, 2016, Detroit, USA*.

[42] J. Puryear, L. Reese, and B. Harrison, "Wear analysis of machinery components in buildings," in *16th International LS-DYNA Users Conference, June 10-11, 2020, Virtual event*.

[43] B. S. Massey, *Mechanics of fluids*. Chapman and Hall, London, UK, 6th ed., 1989.

[44] M. Axin, R. Braun, A. Dell'Amico, B. Eriksson, P. Nordin, K. Pettersson, I. Staack, and P. Krus, "Next generation simulation software using transmission line elements," in *Fluid Power and Motion Control*, (Bath, England), October 2010.

[45] R. Braun, *Distributed System Simulation Methods : For Model-Based Product Development*. PhD thesis, Linköping University, Fluid and Mechatronic Systems, Faculty of Science & Engineering, 2015.

[46] D. M. Auslander, "Distributed system simulation with bilateral delay-line models," *Journal of Basic Engineering*, vol. 90, no. 2, pp. 195–200, 1968.

[47] T. Belytschko, W. K. Liu, B. Moran, and K. Elkhodary, *Nonlinear finite elements for continua and structures*. John Wiley & Sons, 2013.

[48] F. M. White, *Viscous fluid flow*, vol. 3. McGraw-Hill New York, 2006.

[49] L. E. Barrett and E. J. Gunter, "Steady-state and transient analysis of a squeeze film damper bearing for rotor stability," Tech. Rep. CR-2548, NASA, 1975.

[50] A. Haufe, K. Roll, and P. Bogon, "Sheet metal forming simulation with elastic tools in LS-DYNA," in *Proceedings of the 7th International Conference, NUMISHEET*, 2008.

[51] B. Lundberg, *Some basic problems in percussive rock destruction*. PhD thesis, Chalmers University of Technology, Department of Solid Mechanics, Göteborg, 1971.

[52] R. Chacon and M. Ivantysynova, "An investigation of the impact of the elastic deformation of the end case/housing on axial piston machines cylinder block/valve plate lubricating interface," in *Proceedings of the 10th IFK International Conference on Fluid Power, Dresden, Germany*, vol. 1, pp. 283–294, 2016.

Part II

Appended papers

Papers

The papers associated with this thesis have been removed for copyright reasons. For more details about these see:

https://doi.org/10.3384/9789179292096

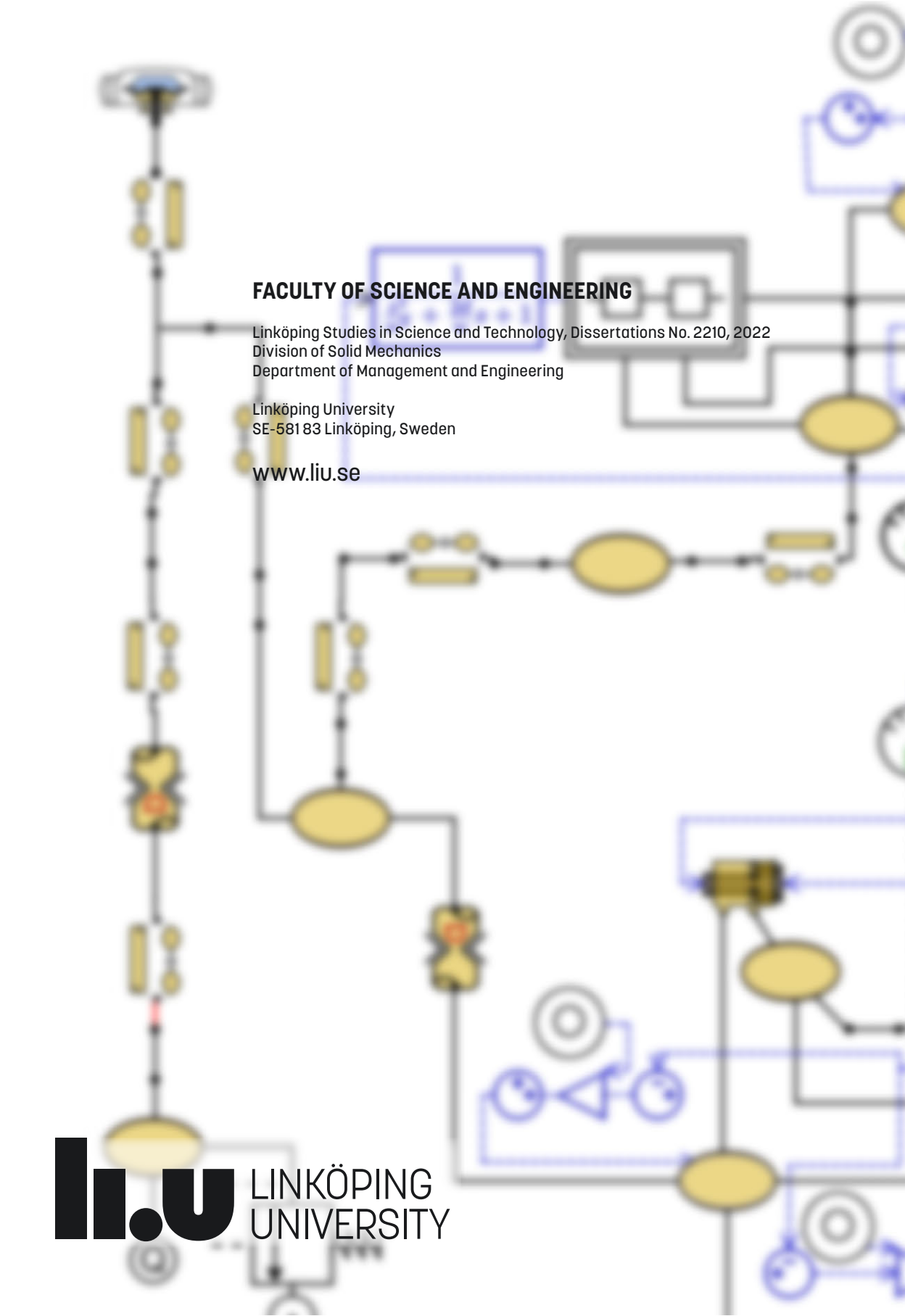

FACULTY OF SCIENCE AND ENGINEERING

Linköping Studies in Science and Technology, Dissertations No. 2210, 2022
Division of Solid Mechanics
Department of Management and Engineering

Linköping University
SE-581 83 Linköping, Sweden

www.liu.se

LINKÖPING UNIVERSITY